SECOND EUROPEAN ROTORCRAFT AND POWERED LIFT AIRCRAFT FORUM

Paper No. 14

SOME ASPECTS OF MECHANICAL INSTABILITY PROBLEMS FOR A FULLY ARTICULATED ROTOR HELICOPTER

PAOLO BELLAVITA

CLAUDIO GIORGI

MASSIMO GALEAZZI

Costruzioni Aeronautiche Agusta
Cascina Costa - Varese - Italy

September 20 - 22, 1976

Buckeburg, Federal Republic of Germany

Deutsche Gesellschaft fur Luft - und Raumfahrt e.V.

Postfach 510645, D-5000 Köln, Germany

ABSTRACT

Self-sustained oscillations due to dynamic coupling between rotary parts and non-rotary parts of a helicopter supported by an elastic and damping landing system are usually referred to as "ground resonance". Oscillations of the blades about their drag hinges cause a displacement of the rotor center of gravity with respect to the axis of rotation generating inertia forces which oscillate at a frequency which is a function of the blade inplane natural frequency and rotor angular velocity. These forces excite the non-rotary parts of the helicopter supplying energy. When the frequency of the rtia forces is tuned with the non-rotary parts n al frequency, then the system resonates. In order to decouple the motions of blades and fuselage, stiffness and damping characteristics of blades and la ar must be properly determined. Coleman wr equations that describe the phenc of ground resonance for small oscillations of blades about their drag hinges, the dynamic characteristics of the fuselage being concentrated in the hub. The subsequent studies made after Coleman have maintained the linearity of the parameters and the schematization of the fuselage at the hub. For a better understanding of the phenomenon of ground resonance we thought it was interesting to use a method that would identify the important physical parameters and consider the non-linearity of these. This method was found to be a useful tool for the design as it permits a direct study of the influence of the constructive parameters on stability. A computer programme simulating hydraulic damper functions is described in this paper and the data thus obtained are compared with experimental results. The results of the dynamic tests performed to investigate the characteristics of different types of elastomeric materials are presented.

LIST OF SIMBOLS

M	= Mass of helicopter
c_L, c_O, c_V	= Long., lat. and vert. damping of oleo-pneumat. system
k_L, k_O, k_V	= Long., lat. and vert. stiffness of oleo-pneum. system
a, b, d, f, g	= Geometrical dimensions of the helicopter
Px, Py	= Force acting on hub in x-y direction
N	= Blades number
m_b	= Blade mass
S_b	= First mass moment of blade about lag hinge
I_b	= Second mass moment of blade about lag ge
e	= Lag hinge offset
$\nu_o = \sqrt{\frac{e \cdot S_b}{I_b}}$	= Non-dimensional blade parameter
C_i	= Lag damping rate of i-th blade
K_i	spring rate of i-th blade
Ω	speed
ω_{oi}	= In-plane natural frequency of i-th blade
ζ_i	= Lag deflection of i-th blade
ψ_i	= Azimuthal location of i-th blade
x_c, y_c	= Coordinates of rotor center of mass
x_h, y_h	= Coordinates of hub
λ	= Ratio between heights of the specimen before and after compression
F'', F'	= Damping and elastic force for elastomer specimen
φ	= Phase angle
K', K''	= Dynamic elastic and damping stiffness of the elastomeric damper
T'_R	= Transmissibility of a vibratory system at resonance
T_R	= Transmissibility of a viscous damped vibratory system
c	= Viscous damping constant
c_{cr}	= Critical damping constant
c_e	= Equivalent viscous damping ratio
F_R	= Reaction force of piston rod
σ	= Coefficient of hydraulic resistence
V_{pist}	= Piston velocity
L, L_1	= Energy absorbed per cycle by the real damper and by equivalent viscous damper
C_{eq}	= Equivalent viscous damping
S	= Useful section of piston
Δp	= Pressure loss across the orifice
C_{eff}	= Flow coefficient
s	= Surface area of the orifice
ρ	= Density of fluid

INTRODUCTION

Coleman (Ref.1), in his studies on the instability of helicopters, assumes that a helicopter on its landing gear system can be represented by a set of effective (equivalent) parameters at the rotor hub. This model lowers the number of degrees of freedom of the system to N+2, that is, the longitudinal and lateral displacements of the hub (fuselage) and the in-plane rotations of the N blades about their drag hinges.
Between each blade and hub there is a damper that has an angular damping coefficient Ci and a spring that has an angular stiffness Ki.
The main characteristics of the Coleman approach to the study of the problem are: two degrees of freedom for the helicopter, linearity (small oscillations and [illegible]s with linear characteristics), isotropy ([illegible]od chosen by Coleman to solve the tions with periodic coefficients utilizes the possible isotropy of the rotor and/or of the pylon to reduce these equations to those with constant coefficients).
Capurso and Gabel (Ref.2), have reduced the number of degrees of freedom of the pylon to just one, have maintained the conditions of linearity and isotropy of Coleman but have simplified the search for the limits of stability for design purposes (utilization of quasi-normal coordinates and Routh method).
Recently Hammond (Ref.3) has studied the problem dismissing the conditions of isotropy and permitting solutions also in the case of one damper inoperative. The concept of the reduction of a helicopter to an equivalent mass and the linearity of the coefficients are retained.
The absence of isotropy does not permit the reduction of a system with periodic coefficients to one of constant coefficients. The Floquet approach provides an efficient means of dealing with this situation.
In the design stage of a helicopter it is necessary first of all to have at our disposal the parameters of the critical components that are responsible for the mechanical instability (Main Rotor Dampers, Dampers and pneumatic tyres of the landing gear system).

It should be interesting to have an engineering method available which permits the writing of the equations of motion with true coefficients of the mechanical components. The model will, therefore, contain physical quantities already known at the design stage and these will not be sought for by actual testing on the helicopter. A scheme of solution has, therefore, been developed which is characterized by the following peculiarities. Equations are derived by the schematization of the helicopter as a rigid body supported on landing gear, non-linearity in the behaviour of the dampers and possibilities of having or not having an isotropy in the rotor. These conditions impose a search for a solution by a step by step integration method with relative description of the time-history.
A most general development of this approach (considering roll and pitch motions) has been judged that is not essential to have results with major precision. We can now have a simplified scheme considering only roll motions which is practical to use.

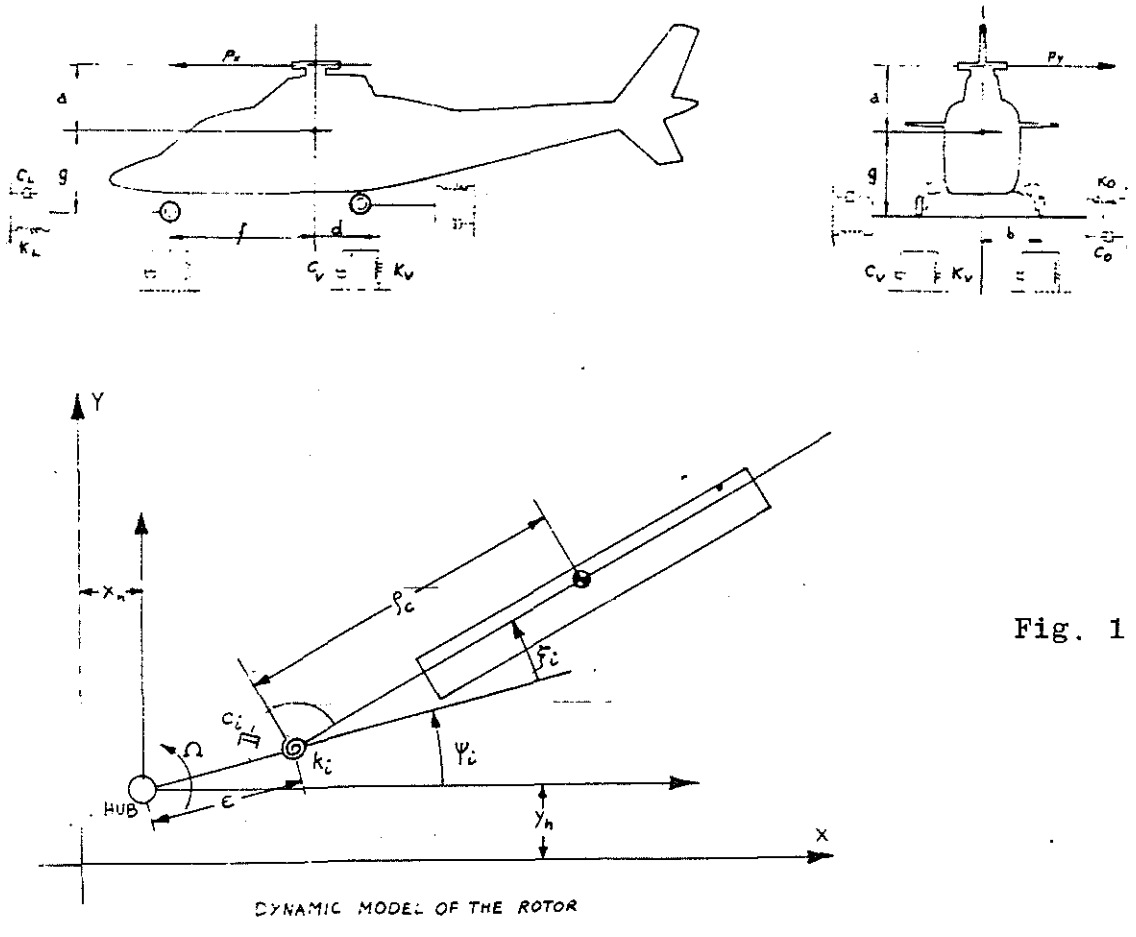

DYNAMIC MODEL OF THE ROTOR

Fig. 1

EQUATIONS OF MOTION

To describe the motion of the fuselage (without the blades) standing on the tyres of the landing gear system, we should consider 6 degrees of freedom -3 translatory and 3 rotatory. On a first approximation we can delete from this scheme the vertical (i.e. along the Z-axis) disturbances and yaw motions.
The experimental results have confirmed that the pitch and roll motions are normally uncoupled and hence can be studied separately even if the equations containing coupled terms should not present any complications in solving them.
The scheme, therefore, will be as that shown i igure 1. with 2 degrees of freedom of translation (c lacements in the x and y axes of the C.G.) plus 2 degrees of freedom of rotation (angular motions of the fuselage around the x and y axes).

$$
\begin{aligned}
&M\ddot{x} + 3K_L x = -3K_L g\varphi - 3c_L g\dot{x} \\
&I_y\ddot{\varphi} + \chi\dot{\varphi} + \beta\varphi = -3K_L g y - 3c_L g\dot{x} - P_x a \\
&\chi = c_v(2d^2+f^2) + 3c_L g^2 \qquad \beta = K_v(2d^2+f^2) + 3K_L g^2
\end{aligned}
\tag{1}
$$

$$
\begin{aligned}
&M\ddot{y} + 2c_o\dot{y} + 2K_o y = -2gK_o\theta - 2gc_o\dot{\theta} + P_y \\
&I_x\ddot{\theta} + \chi\dot{\theta} + \beta\theta = -2gK_o y - 2gc_o\dot{y} - P_y a \\
&\chi = 2(c_o g^2 + c_v b^2) \qquad \beta = 2(K_o g^2 + K_v b^2)
\end{aligned}
\tag{2}
$$

As we can see these equations contain parameters Co, Cv, Ko & Kv which can be determined by a simple calculation at the design stage.
A second approximation could be, as already shown, that of considering just the motions in the yz plane without modifying the general validity of the method and above all its agreement with experiment.
We know that the drag motions of the blades cause a displacement of their C.G. relative to the center of rotation of the hub. The description of this motion can be made by considering all the drag angles as independent variables. This makes the representation of the rotor with one damper inoperative possible.

The equations of motion for the blades are (Fig.1)

$$\ddot{\zeta}_i + \eta_i \dot{\zeta}_i + \left(\omega_{o_i}^2 + \Omega^2 \nu_o^2\right)\zeta = \frac{\nu_o^2}{e}\left(-\ddot{y}_h \cos\psi_i\right) \quad i = 1, .., N \qquad (3)$$

The force that acts on the fuselage along the y-axis due to the motion of the C.G. of the blades is:

$$P_y = -N m_b \ddot{y}_c \qquad (4)$$

The y-coordinate of the C.G. of the blades is:

$$y_c = (R_c/N) \sum_{i=1}^{N} \zeta_i \cos\psi_i \qquad (5)$$

Differentiating twice and substituting in equation (2) above. We get:

$$P_y = -N m_b \ddot{y}_h - S_b \sum_{i=1}^{N} \left[\left(\ddot{\zeta}_i - \Omega^2 \zeta_i\right)\cos\psi_i - 2\Omega\dot{\zeta}\sin\psi_i\right] \qquad (6)$$

The stability of the solution of equations (2) and (6) has been studied by the method of Floquet presented by Hammond (ref.3) and by the method of direct integration (time history).

Observations on the methods of Floquet and Direct Integration

The Floquet method requires the linearity of the parameters; the damper can be linearized with the guide lines described in Appendix A. Normally it is sufficient to choose the Ceq relative to the first minimum of the curve of Ceq Vs piston stroke or peak velocity; the choice of Ceq relative to the x-asymptote may be penalizing. This method is synthetic, does not require a choice of the particular initial conditions and gives directly a measure of the stability of the solutions (damping factor). It is also easy to use, efficient and requires only a short integration time.

The Direct Integration Method is indispensable in the case of non-linear parameters (blade damper) or time-varying parameters (dependence of the elastic and damping characteristics of the landing gear on the condition of airborne while landing) (Fig. 3)

In such a case the stability of the solutions of the non-linear equations can depend on the initial conditions. These initial conditions have to be chosen with care so as to be as near to the actual ones as are used in the simulation. This method, therefore, is not very practical for the verification of the stability. However, this can be used for simulation purposes. In any case the integration time should not be very long.

The studies we have made lead to the following procedure to be adopted at the design stage.

1) Preliminary valuation of the parameters.
2) Determination of the region of instability a function of Rotor RPM and airborne state using the Floquet Method. (Fig.2)
3) Simulation of the instability using the Direct I[illegible]on Method with non-linear paramet[illegible]

If r[illegible] re not satisfactory return to ste[illegible] and examine the parameters.

In appendix A some considerations are cited which demonstrate that Ceq-normally considered a constant in "linear treatment" is seen to be notably influenced by all the physical and geometrical parameters. The possibility of using the real behaviour of the damper, which is non-linear in the calculations for verifying the stability of the helicopter, has prompted the study and the definition of a real model of the damper that might serve for design.

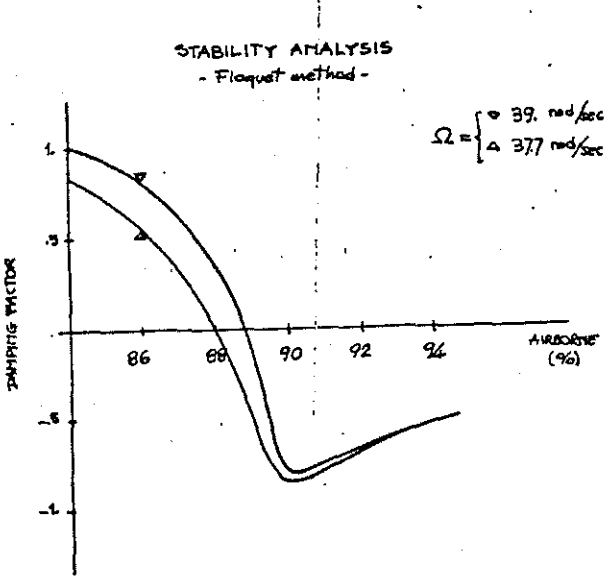

Fig.2

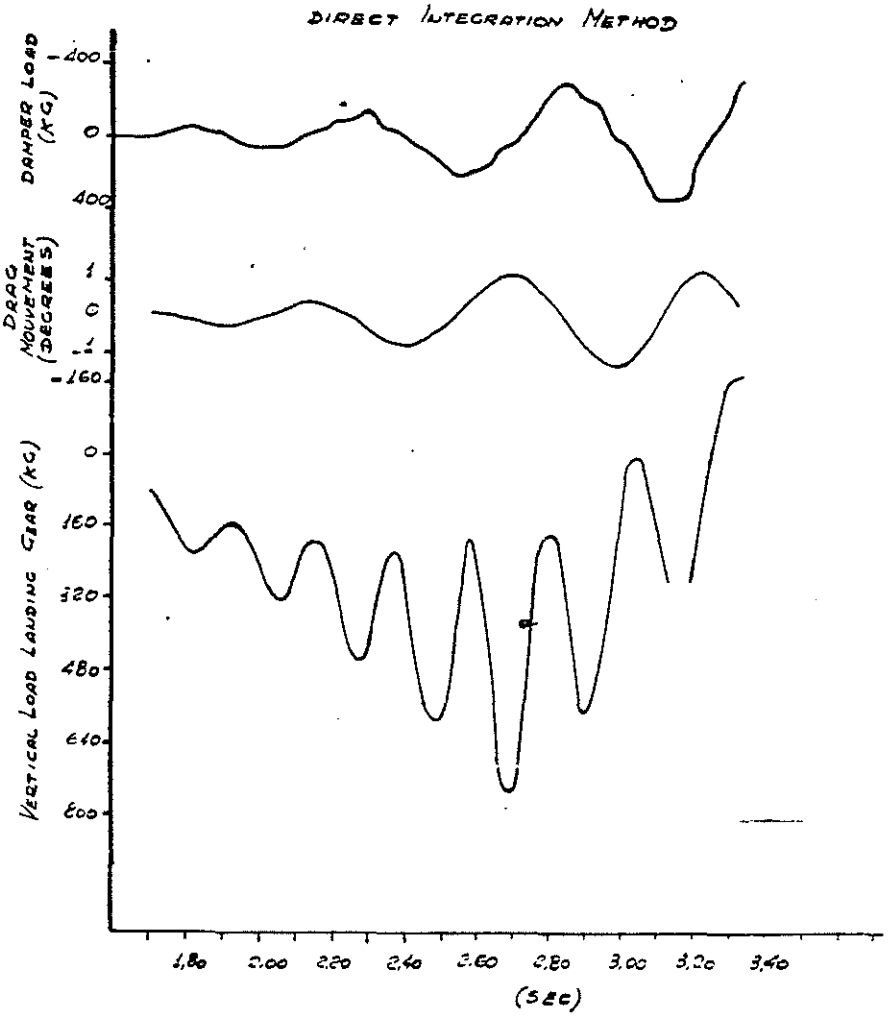
DIRECT INTEGRATION METHOD
DAMPER LOAD (KG)
-400
0
400
DRAG MOUVEMENT (DEGREES)
1
0
-1
-160
0
160
320
480
640
800
VERTICAL LOAD LANDING GEAR (KG)
1,80
2.00
2.20
2,40
2.60
2,80
3.00
3,20
3,40
(SEC)

Fig.3

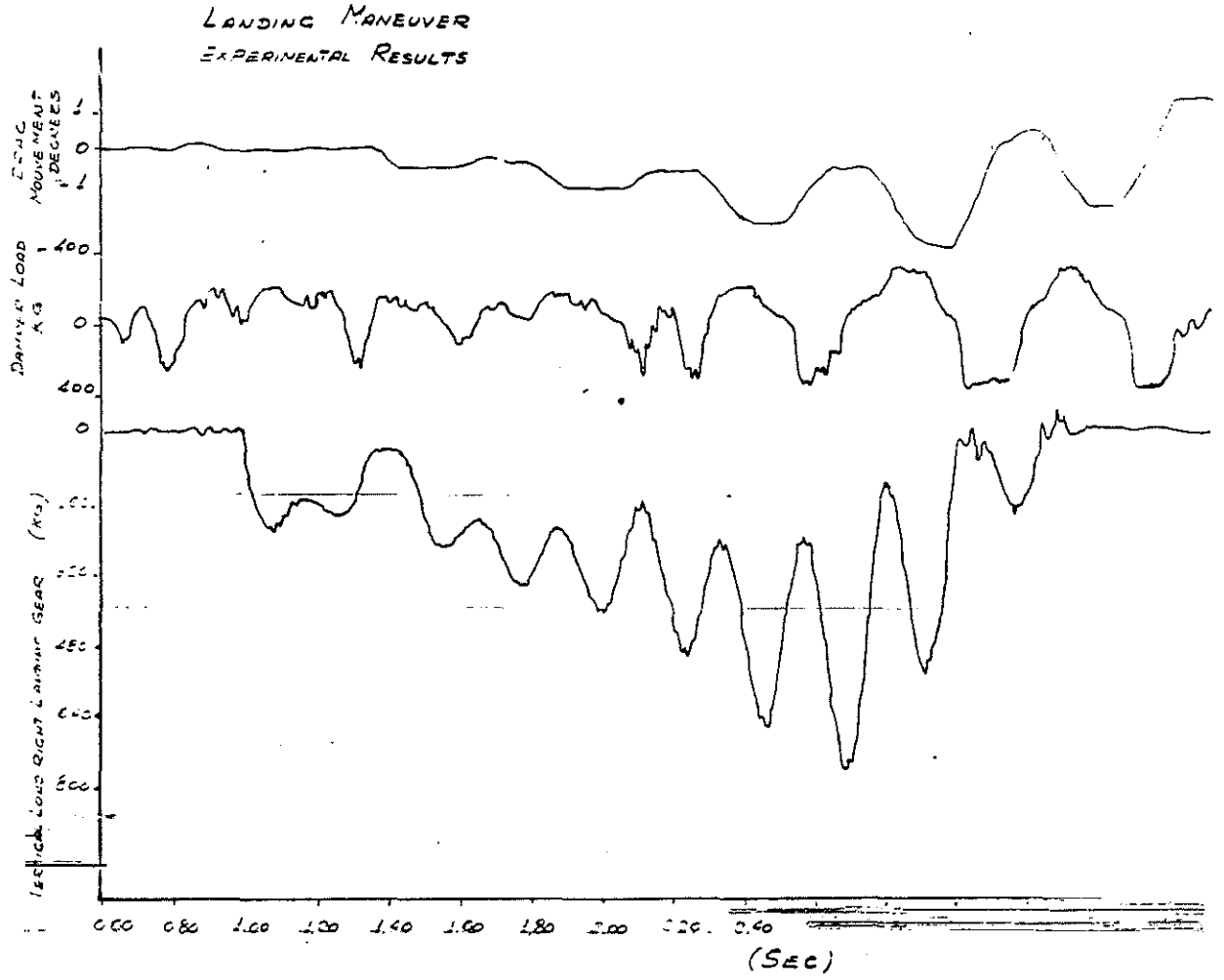
LANDING MANEUVER
EXPERIMENTAL RESULTS
DRAG MOUVEMENT (DEGREES)
1
0
-1
-400
0
400
0
0.00
0.80
1.00
1.20
1.40
1.60
1.80
2.00
2.20
2.40
(SEC)

Fig.4

Theoretical modelling and simulation of a hydraulic damper. Comparison between theoretical and experimental data.

A suitable model of Hydraulic damper was adopted (see Fig. 5) and its behaviour was investigated by systematic variation of the individual component characteristics, like geometry of the system, flow diagram of the valves, support stiffness, spring hysteresis, and so on.
Starting from the equations of the individual elements, a set of differential equations was written describing the whole system. However, solution by means of traditional methods was not possible since some of the coefficients are non-linear scontinuous in their first derivatives, and some behave hysteretically.
The problem was overcome by adopting a method that a s the overall equilibrium by repeated iter n partial equilibrium conditions
In laying out a computer program to implement such a method we considered the highest flexibility as a major requirement and simulation of a damper both on the rig and in-flight, as a goal.
To achieve this, we followed the same philosophy both for the solution method and for programming.
Calculations were performed step by step, the main input being the displacement of the damper rod and equilibrium of flows and loads being the expected solutions.
Calculations consist of three loops, one internal to the other. Initially, values of the elastic displacements and pressures in the chambers are given. After altering the pressure in chamber 1 the program seeks for flow equilibrium in the chamber itself. Then the pressure in chamber 2 is modified and again flow equilibrium in both chambers is looked for. Values for elastic displacements are then determined so as to reach a balance of loads.
The sequence chamber 1 - chamber 2 depends upon the direction of the rod motion. The program block diagram is presented in Fig.7 Input data are geometrical features (stroke, volumes of chambers, etc.), pressure-flow characteristic curves relative to orifices and valves, fluid parameters, support stiffness. Outputs of the program are the time histories of loads, displacements, pressures and work done for a given rod displacement. Data presented here refer to the hydraulic damper defined in Table 1.

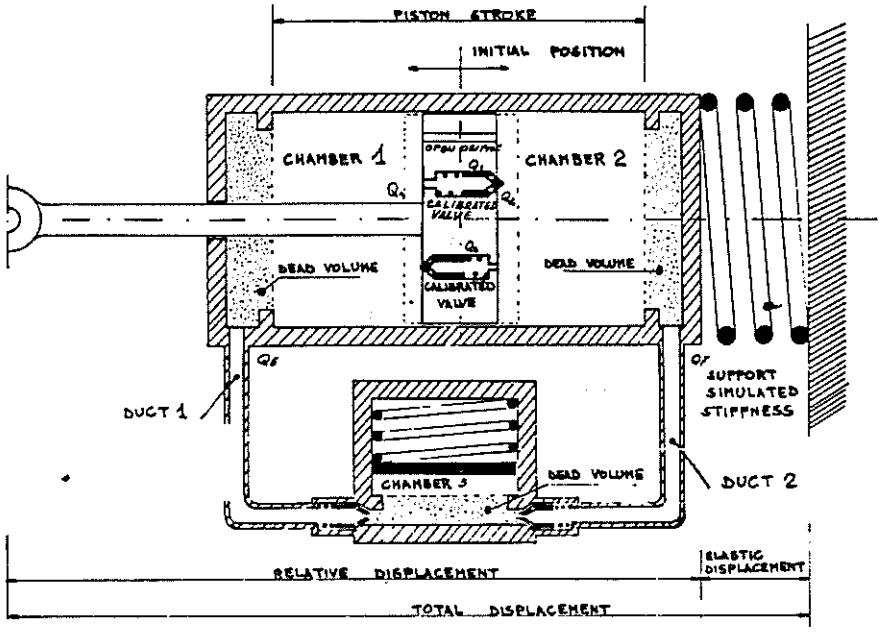
PISTON STROKE
INITIAL POSITION
CHAMBER 1
CHAMBER 2
CALIBRATED VALVE
DEAD VOLUME
DEAD VOLUME
CALIBRATED VALVE
DUCT 1
SUPPORT SIMULATED STIFFNESS
CHAMBER 3
DEAD VOLUME
DUCT 2
RELATIVE DISPLACEMENT
ELASTIC DISPLACEMENT
TOTAL DISPLACEMENT

Fig. 5

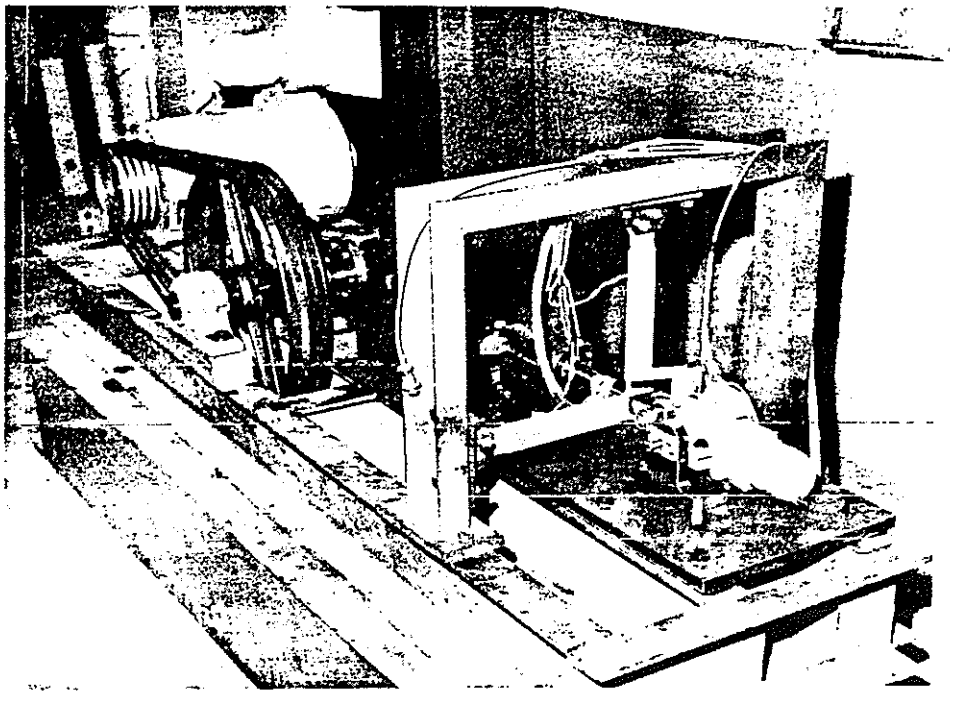

Fig.6

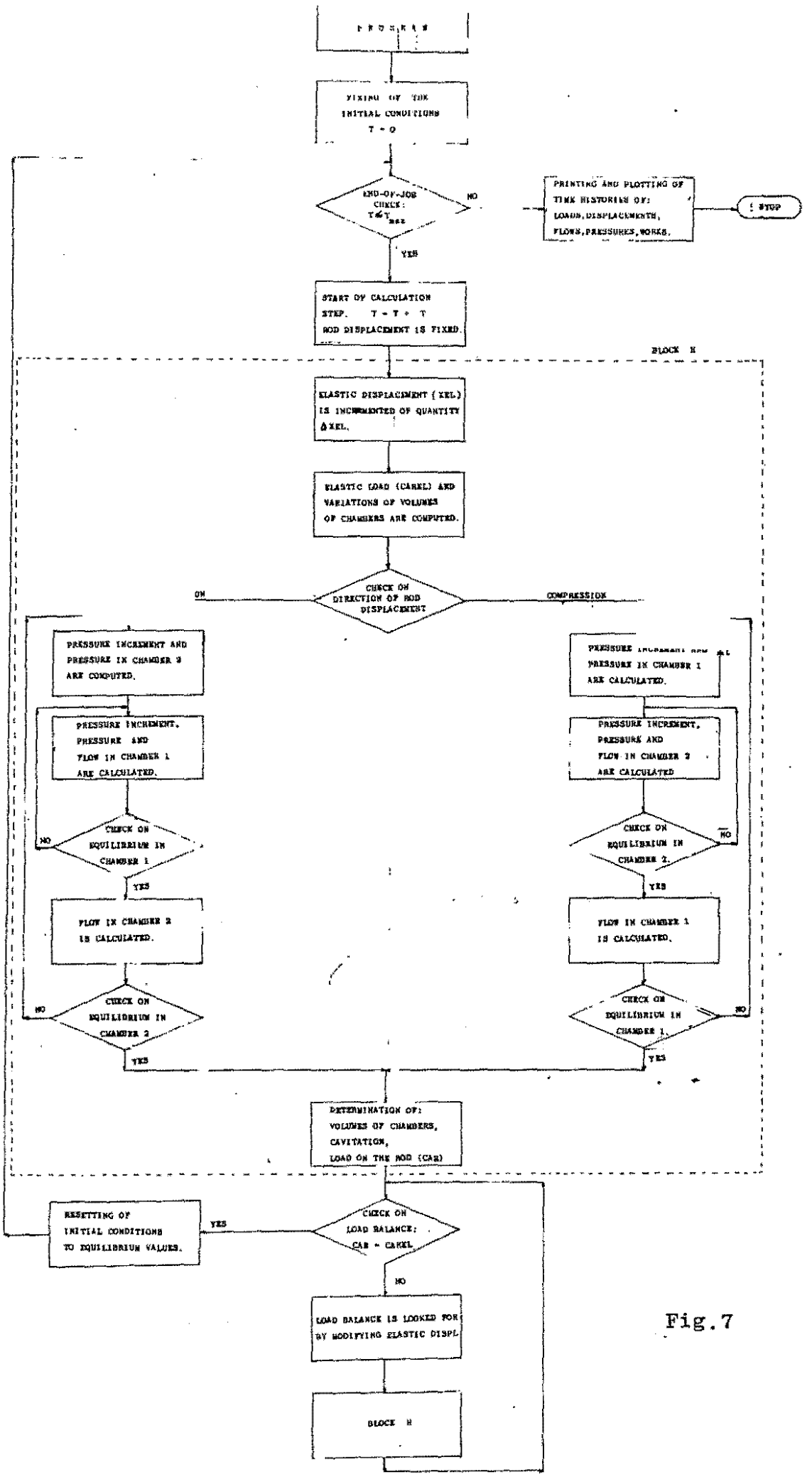
PROGRAM
FIXING OF THE INITIAL CONDITIONS T = 0
END-OF-JOB CHECK: T ≥ T max
NO
YES
PRINTING AND PLOTTING OF TIME HISTORIES OF: LOADS, DISPLACEMENTS, FLOWS, PRESSURES, WORKS.
STOP
START OF CALCULATION STEP. T = T + Δt
ROD DISPLACEMENT IS FIXED.
BLOCK H
ELASTIC DISPLACEMENT (XEL) IS INCREMENTED OF QUANTITY ΔXEL.
ELASTIC LOAD (CAREL) AND VARIATIONS OF VOLUMES OF CHAMBERS ARE COMPUTED.
CHECK ON DIRECTION OF ROD DISPLACEMENT
ON
COMPRESSION
PRESSURE INCREMENT AND PRESSURE IN CHAMBER 2 ARE COMPUTED.
PRESSURE INCREMENT, PRESSURE AND FLOW IN CHAMBER 1 ARE CALCULATED.
CHECK ON EQUILIBRIUM IN CHAMBER 1
NO
YES
FLOW IN CHAMBER 2 IS CALCULATED.
CHECK ON EQUILIBRIUM IN CHAMBER 2
NO
YES
PRESSURE INCREMENT AND PRESSURE IN CHAMBER 1 ARE CALCULATED.
PRESSURE INCREMENT, PRESSURE AND FLOW IN CHAMBER 2 ARE CALCULATED
CHECK ON EQUILIBRIUM IN CHAMBER 2.
NO
YES
FLOW IN CHAMBER 1 IS CALCULATED.
CHECK ON EQUILIBRIUM IN CHAMBER 1.
NO
YES
DETERMINATION OF: VOLUMES OF CHAMBERS, CAVITATION, LOAD ON THE ROD (CAR)
RESETTING OF INITIAL CONDITIONS TO EQUILIBRIUM VALUES.
YES
CHECK ON LOAD BALANCE: CAR = CAREL
NO
LOAD BALANCE IS LOOKED FOR BY MODIFYING ELASTIC DISPL.
BLOCK H

Fig.7

The schematic drawing in Fig. 5 shows two chambers communicating through two orifices, one of them is always open while the other is controlled by a calibrated valve. The characteristic curve of this system (see Fig.8) indicates the opening of the calibrated valve when the differential pressure between the two chambers is 7.2 Kg/cm^2, corresponding to a flow of 20 cm^3/sec.

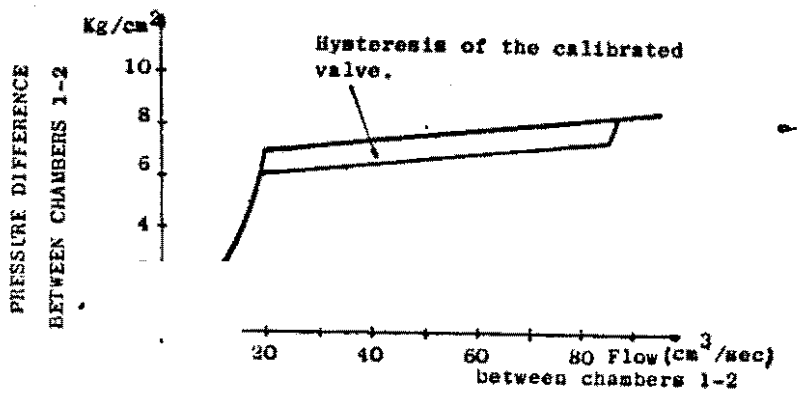

Fig.8

Both chambers communicate through ducts 1 and 2 with a third chamber that works as a pressure limiter. Two partial-check valves are located at the entrance of chamber 3. Fig. 9 shows the relative characteristic curve.

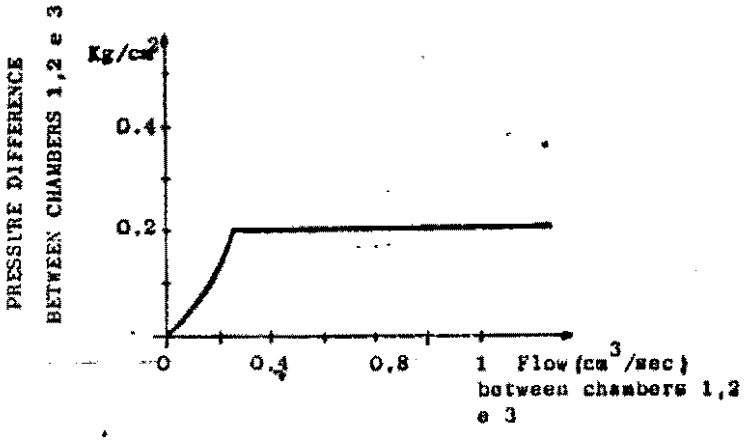

Fig.9

The model of the damper was made by considering all main components that contribute to determine the system behaviour. In the equations layout we also allowed for the possibility of cavitation phenomena during damper operation.
To improve the model, support stiffness was also evaluated. In fact, the reported data indicate that this element plays an important role with regard to negative work which reduces damper effectiveness.
The program also allows for support clearance and valve hysteresis, factors that alter damper operation. The program drew a set of plots (Fig.10) through 13) that have to be related to the list of parameters of Table 2.

Input Data

er Geometry

Chamber 1 Section	33.180 (CM.s2)
Chamber 2 Section	33.180 -
Chamber 3 Section	30.580 -
Chamber 1 Dead Volume	10.000 (CM.s3)
Chamber 2 Dead Volume	5.000 -
Piston Stroke	3.850 (CM.)
Overall Piston Stroke of Chamber 3	6.500 (CM.)
Initial Cavitation Volume in Chambre 1	0.0 (CM.s3)
Initial Cavitation Volume in Chambre 2	0.0 -
Initial Total Displacement	0.0 (CM.)

Pressures

Preload Pressure in Chambre 3	2.000 (KG./CM.s2)

Chambre 3 Valve Characteristics

Chambre 3 Spring Constant	4.070 (KG./CM.)
Spring Maximum Length	12.520 (CM.)

Times

Time Increment	0.00050 (SEC.)
Maximum Time	0.25 (SEC.)

Displacements characteristics

Frequency	8.400 (HZ.)
Initial Displacement (XO)	0.120 (CM.)
Initial Displacement (XIO)	0.0 (CM.)

Table 1

TABLE 2

FINAL CHARACTERISTICS

No.of diagram	Type of motion	Backlash	Hysteresis of the calibrated valve Kg/cm^2	Elasticity of the support Kg/cm	Preload in chamber 3 Kg/cm^2	Activation pressure of calibrated valve Kg/cm^2	Freq.of motion,Hz.	Elastic Constant of spring, in chamber 3 Kg/cm
1	sinusoidal	0	0	30000	2	7.2	8.47	4.07
2	sinusoidal	± 0,025	0	30000	2	7.2	8.61	4.07
3	sinusoidal	± 0,025	1	30000	2	7.2	8.41	4.07
4	sinusoidal	± 0,025	1	8000	2	7.2	8.41	4.07

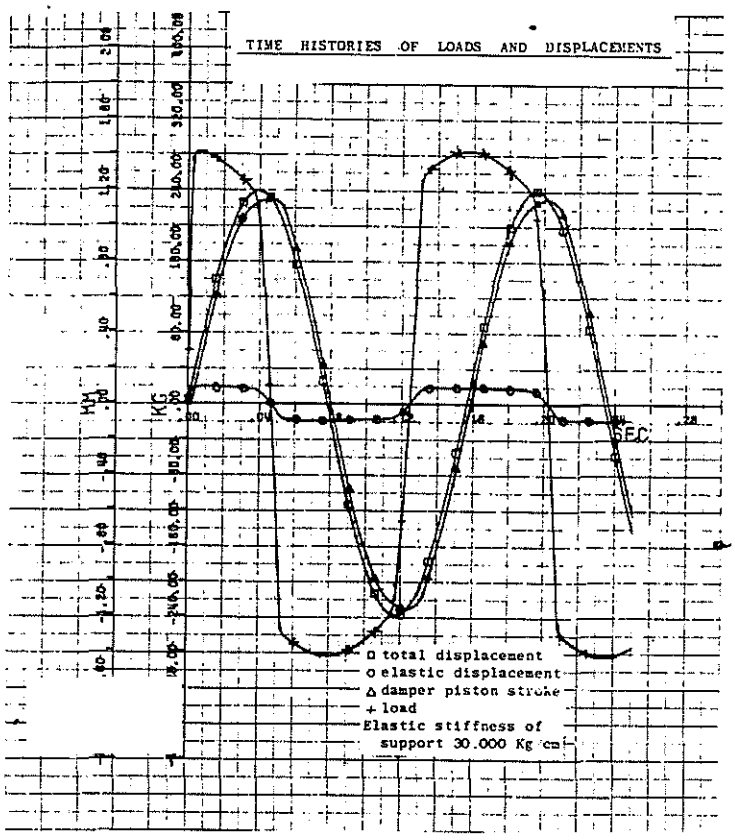
TIME HISTORIES OF LOADS AND DISPLACEMENTS
KN
KG
SEC
□ total displacement
○ elastic displacement
Δ damper piston stroke
+ load
Elastic stiffness of
support 30.000 Kg/cm

Fig. 10

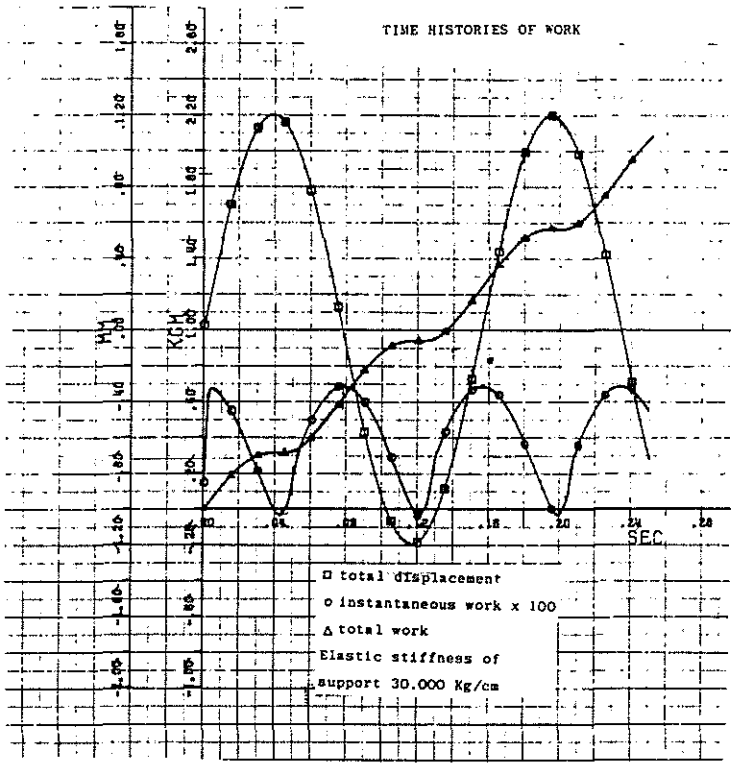
TIME HISTORIES OF WORK
KN
KGM
SEC
□ total displacement
○ instantaneous work x 100
Δ total work
Elastic stiffness of
support 30.000 Kg/cm

(b)

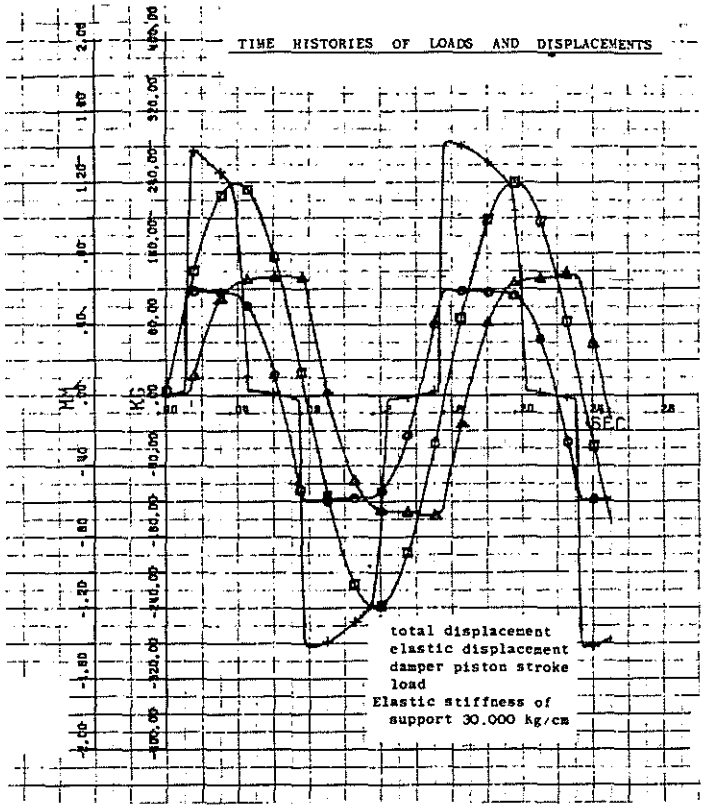
TIME HISTORIES OF LOADS AND DISPLACEMENTS
KG
MM
SEC
total displacement
elastic displacement
damper piston stroke
load
Elastic stiffness of
support 30.000 kg/cm

(a)

Fig. 11

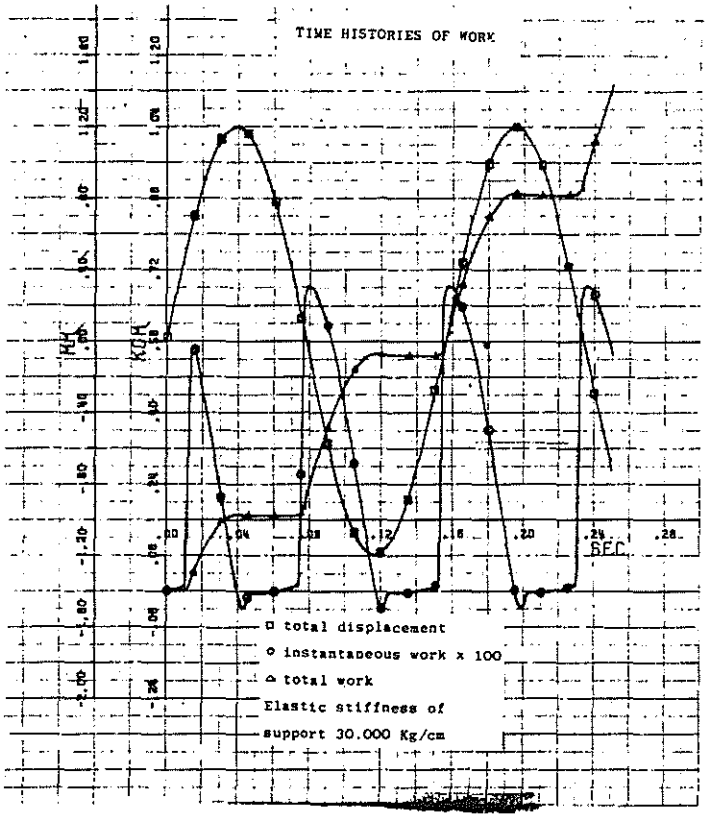
TIME HISTORIES OF WORK
KGM
MM
SEC
total displacement
instantaneous work x 100
total work
Elastic stiffness of
support 30.000 Kg/cm

(b)

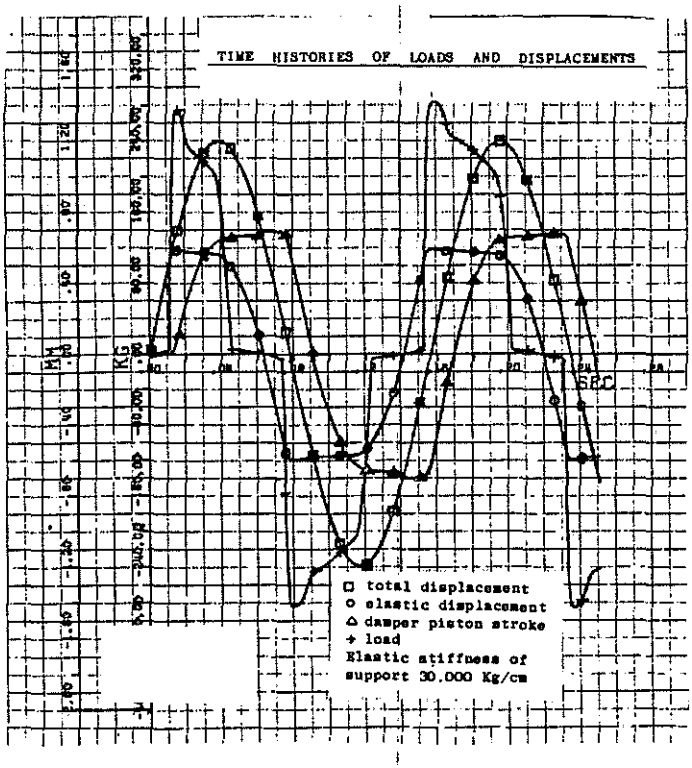
TIME HISTORIES OF LOADS AND DISPLACEMENTS
SEC
□ total displacement
○ elastic displacement
△ damper piston stroke
+ load
Elastic stiffness of
support 30.000 Kg/cm

Fig. 12

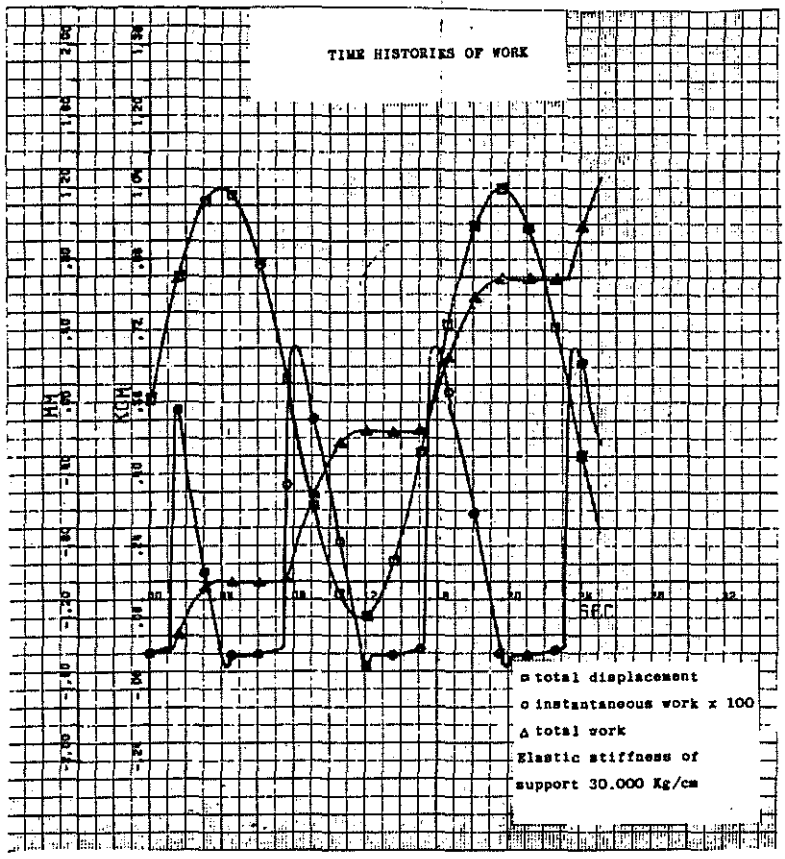
TIME HISTORIES OF WORK
SEC
□ total displacement
○ instantaneous work x 100
△ total work
Elastic stiffness of
support 30.000 Kg/cm

(b)

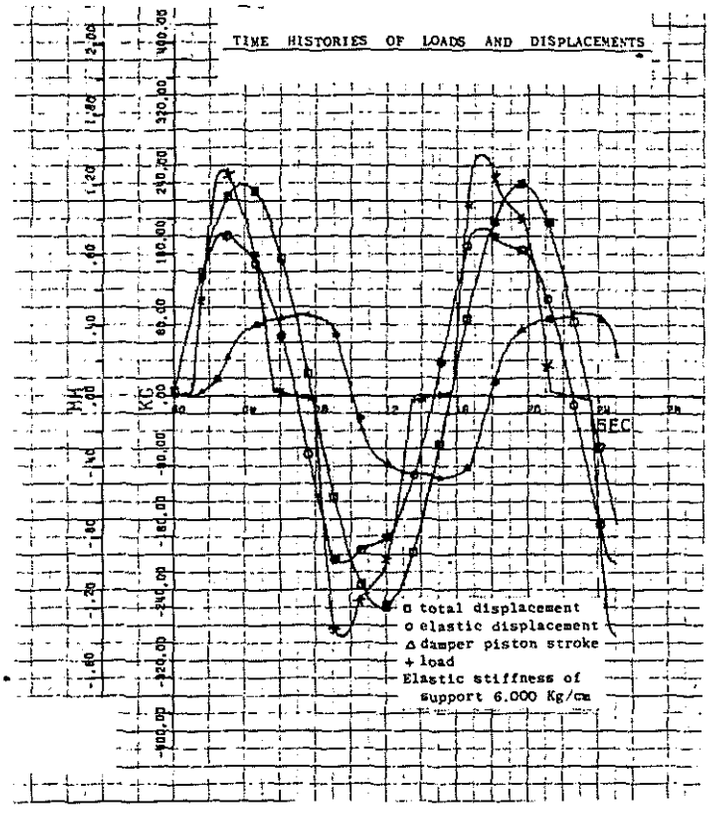
TIME HISTORIES OF LOADS AND DISPLACEMENTS
KG
SEC
□ total displacement
○ elastic displacement
△ damper piston stroke
+ load
Elastic stiffness of
support 6.000 Kg/cm

(a)

Fig. 13

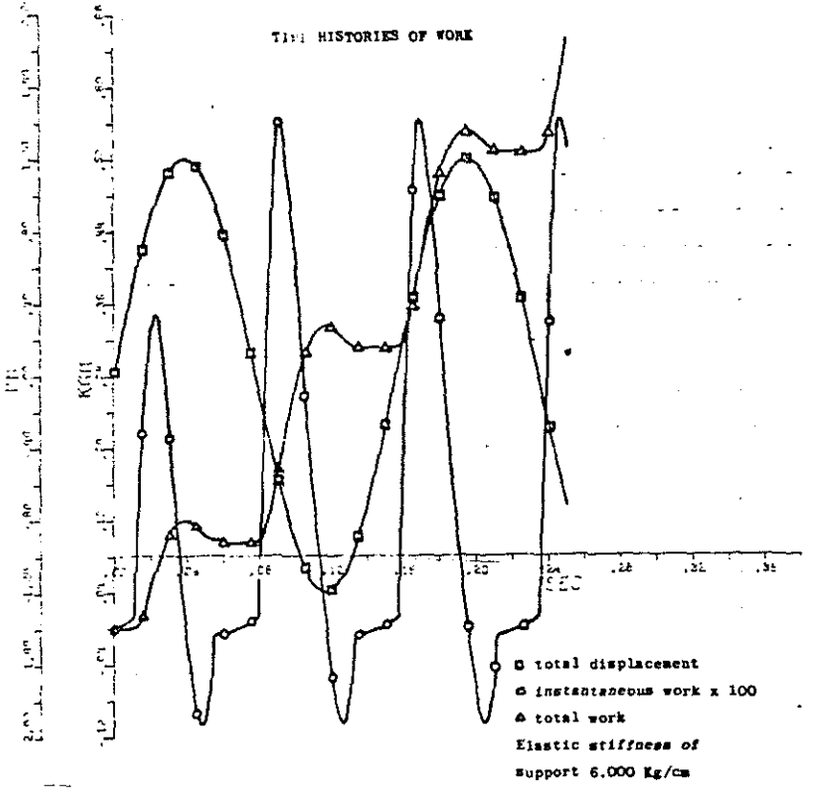
TIME HISTORIES OF WORK
KGM
SEC
□ total displacement
○ instantaneous work x 100
△ total work
Elastic stiffness of
support 6.000 Kg/cm

(b)

With reference to Fig.11(a)-13(a) hysteresis of the spring in the calibrated valve between chambers 1 and 2 causes a peak load whenever the valve opens.
An interesting comparative analysis was also made on work. First of all, looking at the diagrams of Fig.13b and 12b, which differ only by the numerical value of the support stiffness, we notice that negative work decreases considerably as the support stiffness increases. Besides, work per cycle was calculated to be:

1.25	Kg m	without considering any hysteresis or backlash
0.72	Kg m	considering backlash but no hysteresis
0.712	Kg m	considering backlash and hysteresis

The validity of schematization was experimentally verified b ling a hydraulic damper on the particular g shown in Fig. 6. Using the sam values for backlash and hysteresis as used in the computer program, the test results were found to be similar to the calculated ones. (See Fig. 14).
The program made it also possible to optimize damper efficiency; in fact, some parameters were modified and simulation of the modified damper indicate improved performance. As the discrepancies between theoretical data and experimental results were extremely small the program was taken as an excellent design tool for hydraulic dampers.
A refinement of the program (now in its final stage) allows simulation of a damper by taking into account inertia of valves tipical of in flight behaviour.

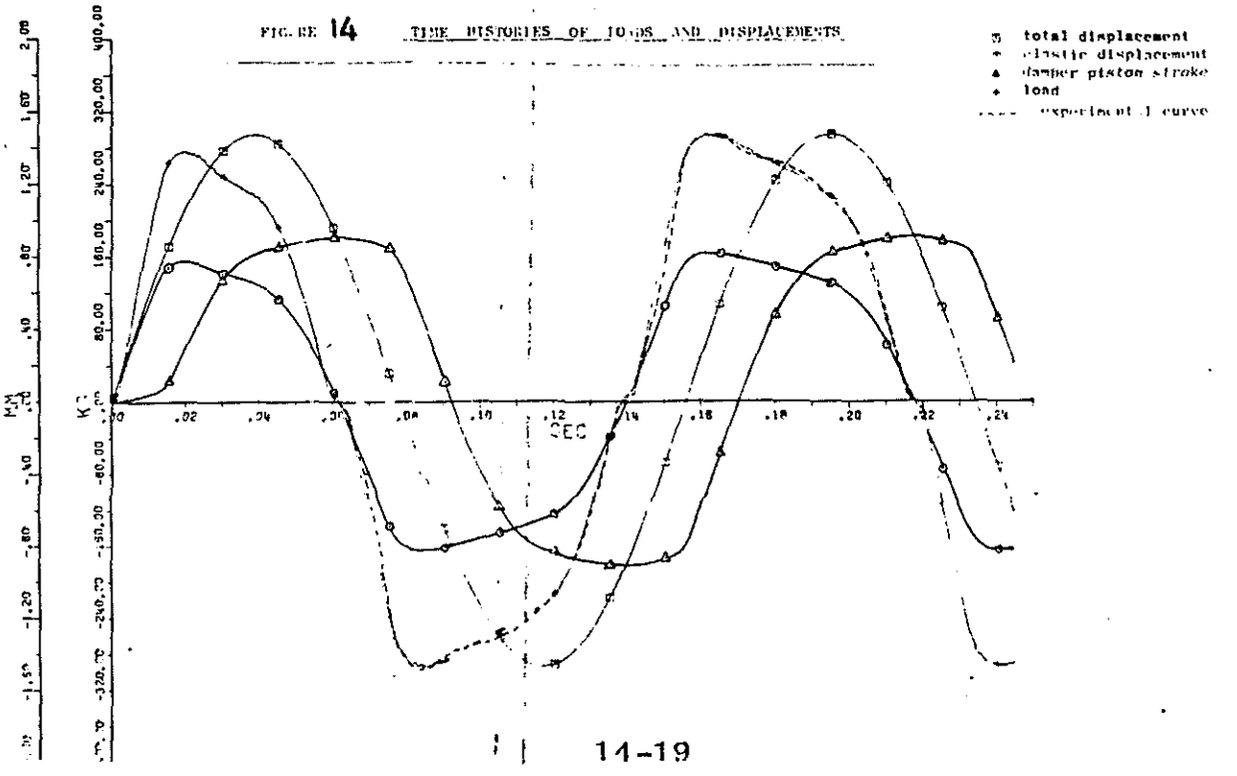

Investigations on Elastomeric Materials for dampers

An analysis of the stability of a helicopter shows that if at the drag hinge, instead of zero moment we have a finite value for K, the natural frequency of the blade in lead-lag increases and simultaneously the blade and landing gear (tyres) damping values necessary for stability decrease.
It is, therefore, logical to think of an elastomeric damper which besides guaranteeing an increased service life and "on condition" performance, also furnishes a stabilising moment and sufficient capacity of damping (Ref. 4-5).
Also as the failure of a damper can bring in instability of the helicopter when operating on ground it is of great interest to study the use of dampers exhibiting peculiar features that help to reduce to a minimum probability of a failure.
Elastomeric dampers seem to have such an advantage; however, we have to cope with an irregular behaviour of the elastomeric material at low frequencies. As a matter of fact, below 20 Hz mechanical characteristics of elastomers show a non-linear relationship with frequency (Ref.4).
The tests described below were performed to study this anomalous behaviour and the influence of orthogonal compression on the performance of different elastomers.
Empirical formulae have been used to determine dimensions of the elastomeric material in the damper.
Elastomers with different hardiness were tested (hardness was measured in IRH units, International Rubber Hardness).
To determine the stiffness of an elastomer the shear stress has to be considered.

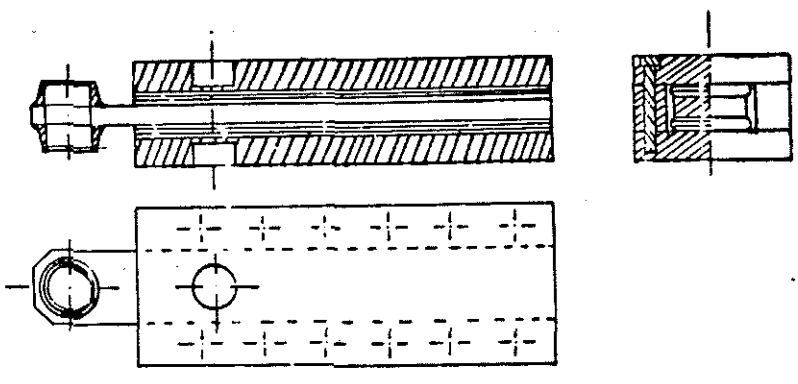

Fig.15

Shear is defined as a stress that causes a displacement of two parallel faces of a test piece, keeping them parallel to each other and at the same distance.

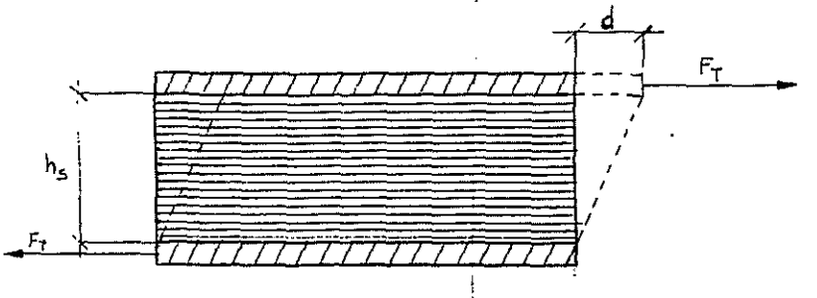

Actually, shear stress is always associated with flexural stress, so that the shear modulus appears to be less than if really is; We took this into account by introducing into the stress-strain formula, a correctio which is a function of the test piece geome refore, the required force to deform a small block of material through by shear is:

$$F_T = A \cdot G \cdot \frac{d}{h_s (1 + h_s^2 / 36\, \rho_{in}^2)}$$

where:

A = section area (cm^2)

G = shear modulus ($Kg\ cm^{-2}$)

ρ_{in} = radius of inertia of the section relative to the flexural neutral axis (cm^2)

h_s = thickness of elastomeric material (cm)

The relationship of shear modulus-hardness is shown in Fig. 16.

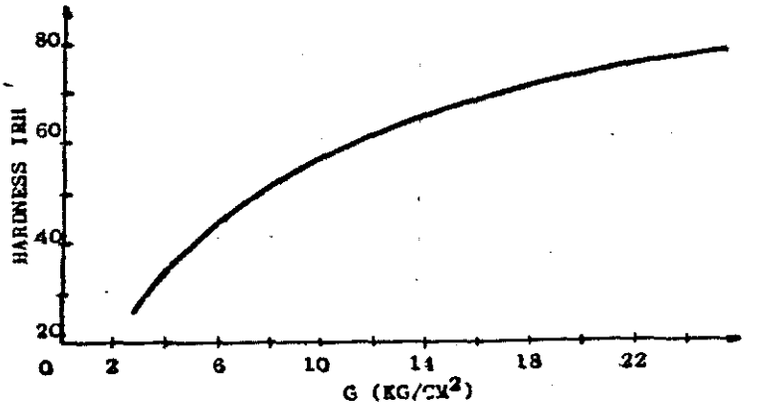

Fig.16

RUBBER (IRH)	APPLIED LOAD (Kg)	w (cm)	l (cm)	INITIAL h before compr. (cm)	FINAL h after compr. (cm)	THEORETICAL d (mm)	ACTUAL d (mm)
48	50	3.3	19.2	0.95	0.75	0.42	0.29
48	100	3.3	19.2	0.95	0.75	0.84	0.625
48	150	3.3	19.2	0.95	0.75	1.26	1
48	200	3.3	19.2	0.95	0.75	1.69	1.38
48	250	3.3	19.2	0.95	0.75	2.11	1.74
48	300	3.3	19.2	0.95	0.75	2.536	2.17

Tabella 3

RUBBER (IRH)	APPLIED LOAD (Kg)	w (cm)	l (cm)	INITIAL h before compr. (cm)	FINAL h after compr. (cm)	THEORETICAL d (mm)	ACTUAL d (mm)
46	50	3.3	19.2	0.95	0.7	0.394	0.24
48	100	3.3	19.2	0.95	0.7	0.789	0.54
48	150	3.3	19.2	0.95	0.7	1.183	0.874
48	200	3.3	19.2	0.95	0.7	1.578	1.199
48	250	3.3	19.2	0.95	0.7	1.972	1.524
48	300	3.3	19.2	0.95	0.7	2.367	1.851

Tabella 4

To determine the load that can be applied to the damper rod of an elastomeric specimen under compressive strain we have to determine the compression force F_c and this can be calculated from:

$$F_c = -G \cdot \left(\lambda - \frac{1}{\lambda^2}\right) \cdot R \cdot A$$

where:

λ = ratio between heights of the specimen before and after compression

G = shear modulus

A = area of the contact surface

$$R = \frac{1.33 + 0.66.(w/l) + C.(w/h)^2}{1 + w/l}$$

Values for coefficient C are given in the following table: (Ref.6)

G	7	7-10.5	10.5-14	14-21	21
C	0.260	0.225	0.175	0.140	0.120

By applying these formulae to the case of a damper with two layers of elastomeric material, we obtained data about strains both from calculations and from experimental tests. The agreement between the two sets of data was acceptable.

RUBBER (IRH)	APPLIED LOAD (Kg)	w (cm)	l (cm)	INITIAL h before compr. (cm)	FINAL h after compr. (cm)	THEORETICAL d (mm)	ACTUAL d (mm)
55	100	3	19.2	0.95	0.7	0.67	0.62
55	200	3	19.2	0.95	0.7	1.35	1.44
55	300	3	19.2	0.95	0.7	2.02	2.33
55	400	3	19.2	0.95	0.7	2.7	3.33
55	500	3	19.2	0.95	0.7	3.37	4.31
55	600	3	19.2	0.95	0.7	4.05	4.65

Tabella 5

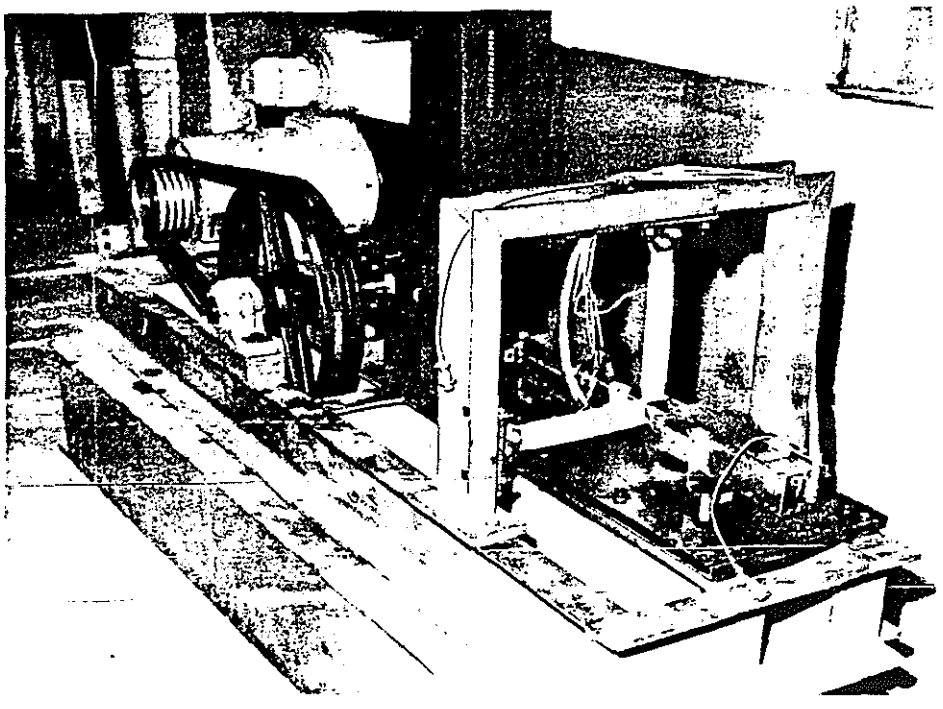

Fig.17

When designing an elastomeric damper, the hysteresis of the material and the relationship between frequency and damping must be known.
In fact, because of the particular molecular structure, when an elastomeric material is deformed, a hysteresis phenomenon occurs due to internal friction. For sinusoidal displacements this internal friction causes a phase shift between load and displacement.
According to the basic information contained in Ref.4 the total force that we record can be represented as a vector consisting of two components, one in-phase with the strain, the other 90° out of phase

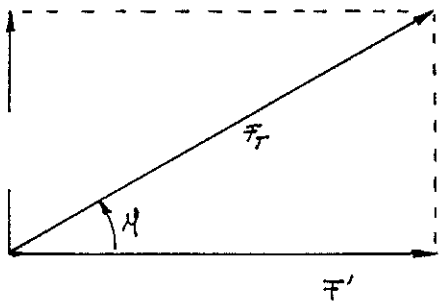

F'' = damping force

F' = elastic force

F_T = total resisting force

Values of F_T and φ depend upon the amplitude of the damper rod displacement x, dimensions and type of the elastomer. We can define:

F'/x = K' = dynamic elastic stiffness of the elastomeric damper

F''/x = K'' = damping stiffness of the elastomeric damper

x being the displacement amplitude.
Dynamic characteristics are expressed by the equivalent viscous damping ratio:

$$c_e = \frac{c}{c_{cr}}$$

where,

c = viscous damping constant

c_{cr} = critical damping constant

Such a ratio can be easily calculated provided parameters K' and K'' are known. In fact, transmissibility T'_R of a vibratory system operating at resonance, is given by the relationship:

$$T'_R = 1 + \left(\frac{1}{(K''/K')}\right)^2$$

equating the two expressions of the transmissibility relative respectively to a viscous-damped vibratory system operating at a frequency f and to the same expression when the system is at resonance, we have:

$$1 + \frac{1}{(K''/K')^2} = \frac{1 + (2.c/c_{cr})^2}{4.(c/c_{cr})^2}$$

By setting = Q, The Quality Factor

then:

$$\frac{c}{c_{cr}} = \frac{1}{2.Q}$$

Operating with the special rig pictured in Fig.17 a set of tests was performed on rubbers with various IRH at different compression stress levels and different amplitudes of rod displacements.

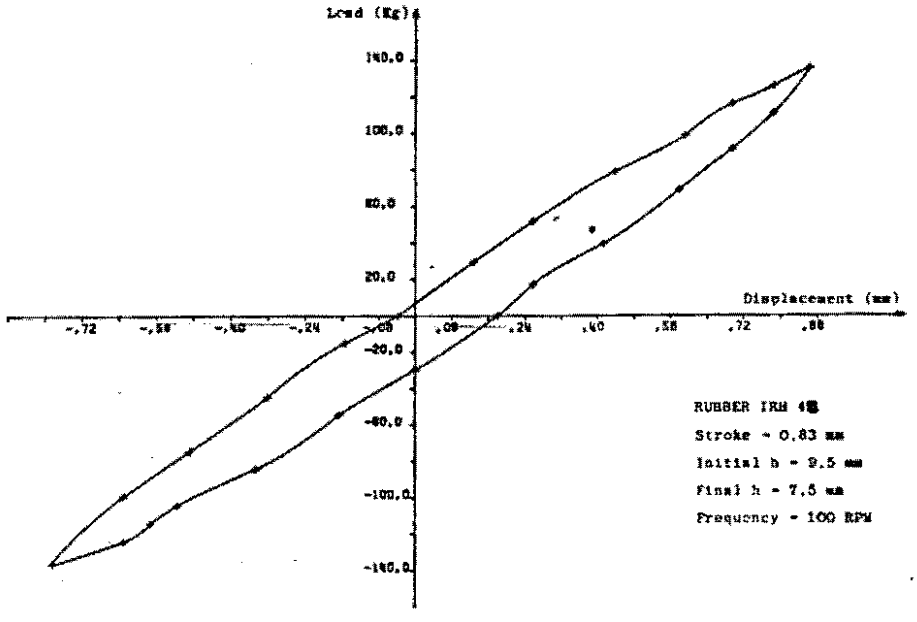

Fig.18(a)

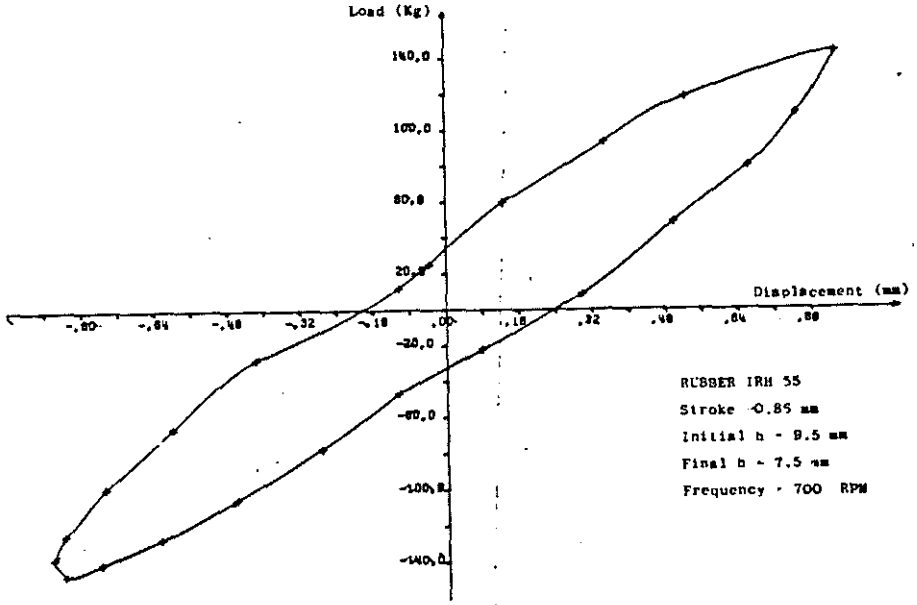
Load (Kg)
Displacement (mm)
RUBBER IRH 55
Stroke -0.85 mm
Initial h - 9.5 mm
Final h - 7.5 mm
Frequency - 700 RPM

(b)

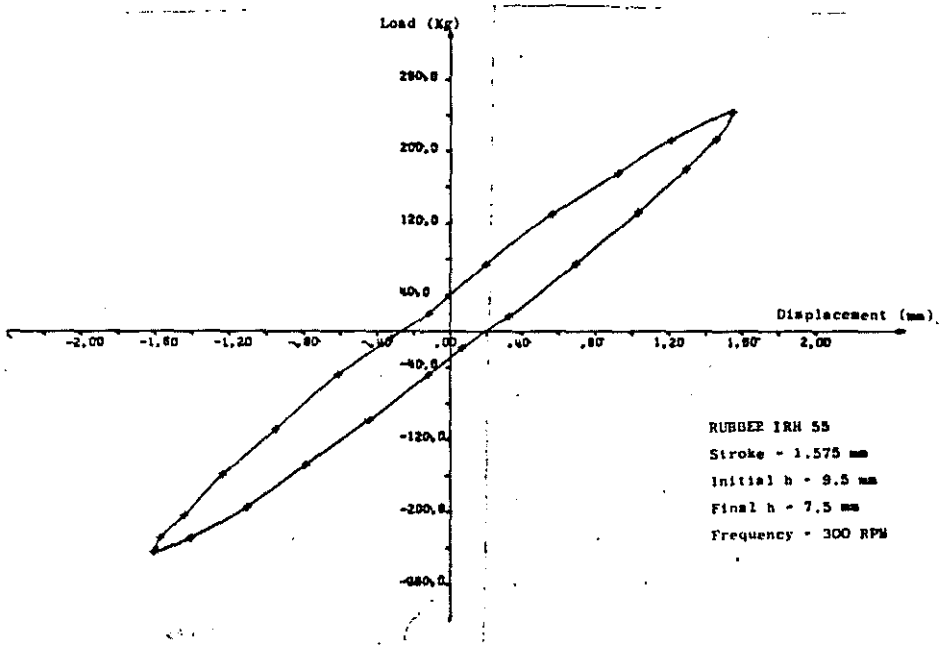
Load (Kg)
Displacement (mm)
RUBBER IRH 55
Stroke - 1.575 mm
Initial h - 9.5 mm
Final h - 7.5 mm
Frequency - 300 RPM

(c)

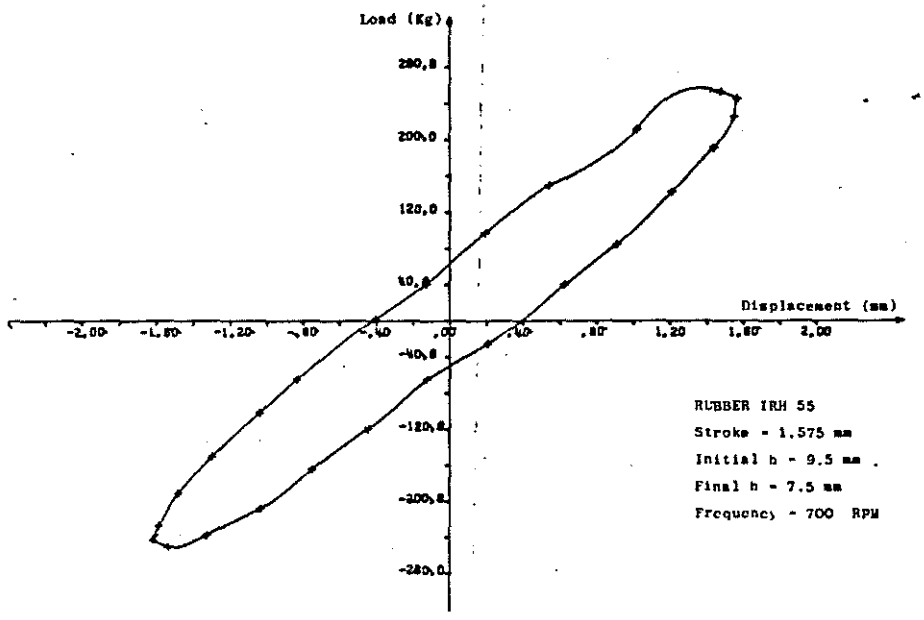
Load (Kg)
Displacement (mm)
RUBBER IRH 55
Stroke - 1.575 mm
Initial h - 9.5 mm
Final h - 7.5 mm
Frequency - 700 RPM

(d)

Fig.18

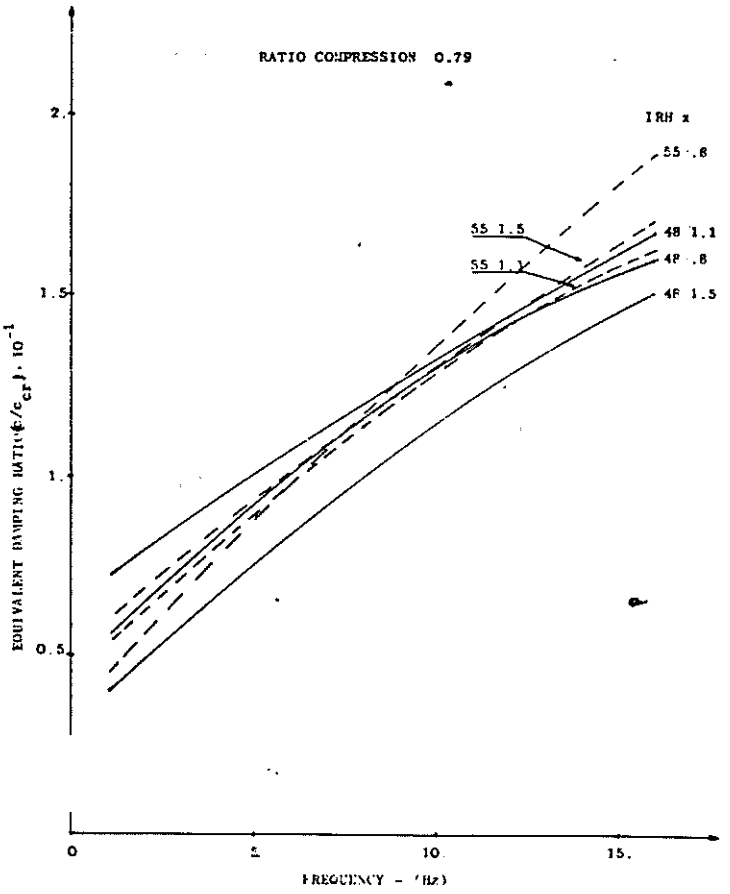
RATIO COMPRESSION 0.79
IRH x
55 .8
55 1.5
48 1.1
55 1.1
4P .8
4P 1.5
2.
1.5
1.
0.5
0
5
10
15.
FREQUENCY - (Hz)

(a)

Fig. 19

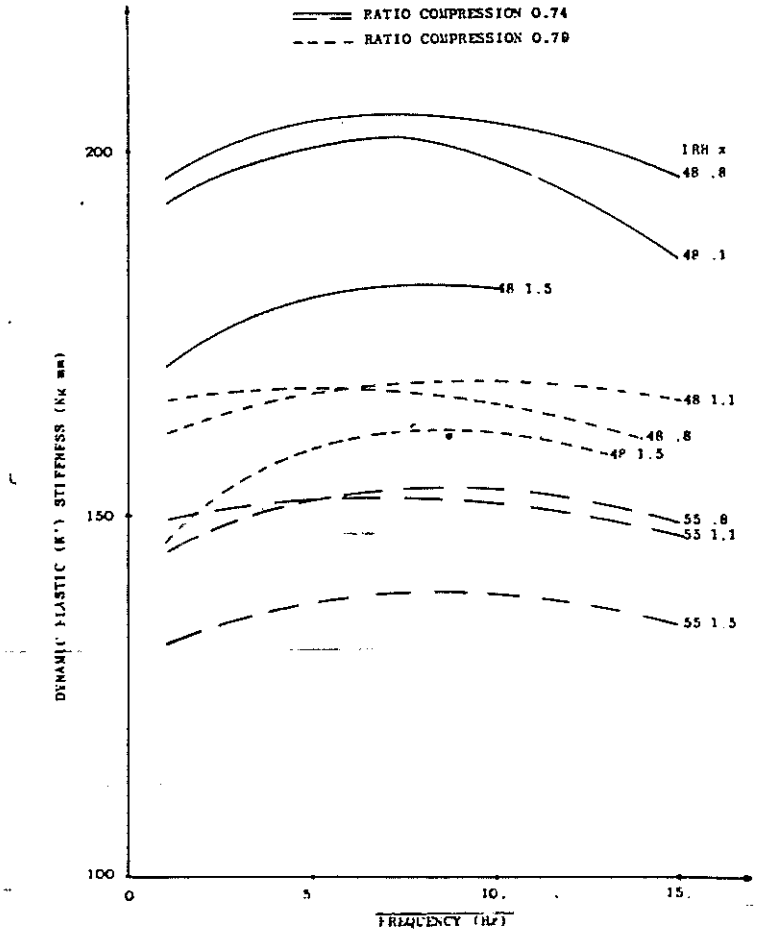
RATIO COMPRESSION 0.74
RATIO COMPRESSION 0.79
IRH x
48 .8
4P .1
48 1.5
48 1.1
48 .8
4P 1.5
55 .8
55 1.1
55 1.5
200
150
100
0
5
10.
15.
FREQUENCY (Hz)

(b)

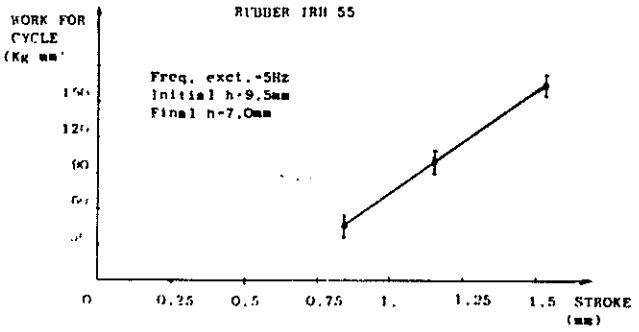
RUBBER IRH 55
WORK FOR CYCLE (Kg mm)
Freq. exct.=5Hz
Initial h=9.5mm
Final h=7.0mm
0
0.25
0.5
0.75
1.
1.25
1.5
STROKE (mm)

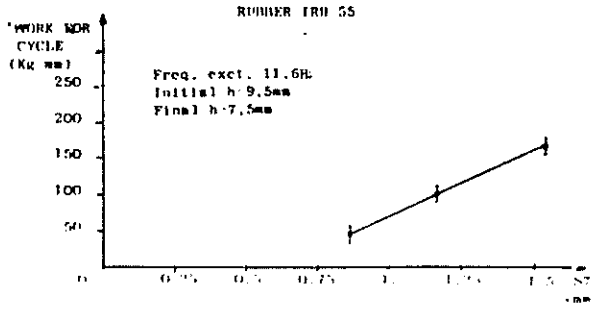
RUBBER IRH 55
WORK FOR CYCLE (Kg mm)
Freq. exct. 11.6Hz
Initial h=9.5mm
Final h=7.5mm
250
200
150
100

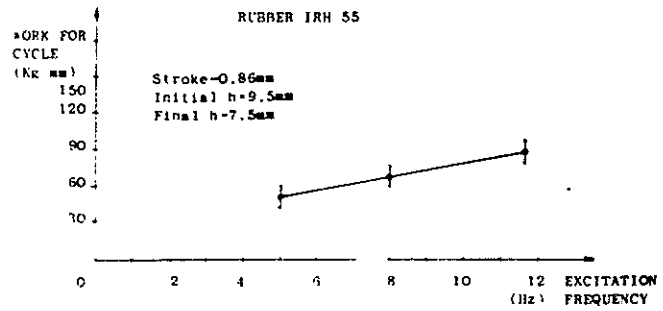
RUBBER IRH 55
WORK FOR CYCLE (Kg mm)
Stroke=0.86mm
Initial h=9.5mm
Final h=7.5mm
150
120
90
60
0
2
4
6
8
10
12
EXCITATION FREQUENCY (Hz)

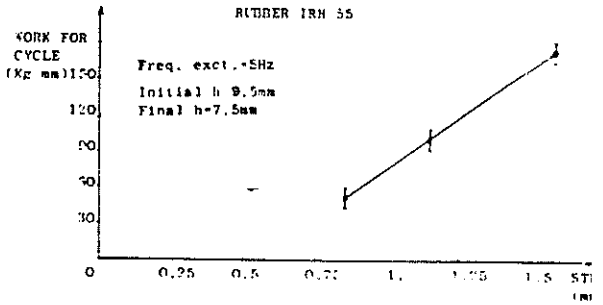
RUBBER IRH 55
WORK FOR CYCLE (Kg mm)
Freq. exct.=5Hz
Initial h=9.5mm
Final h=7.5mm
150
120
90
60
30
0

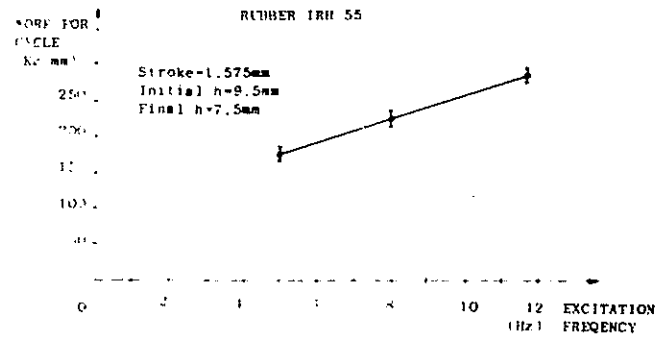
RUBBER IRH 55
Stroke=1.575mm
Initial h=9.5mm
Final h=7.5mm
0
10
12
EXCITATION FREQENCY (Hz)

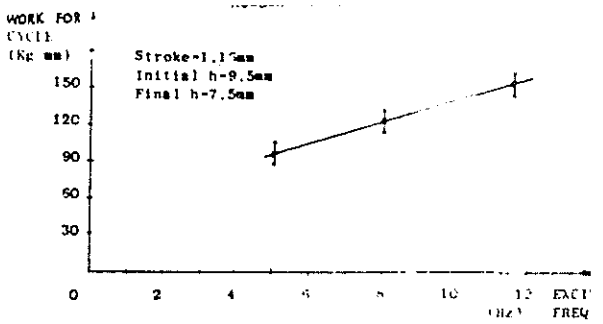
WORK FOR CYCLE (Kg mm)
Stroke=1.1
Initial h=9.5mm
Final h=7.5mm
150
120
90
60
30
0
2

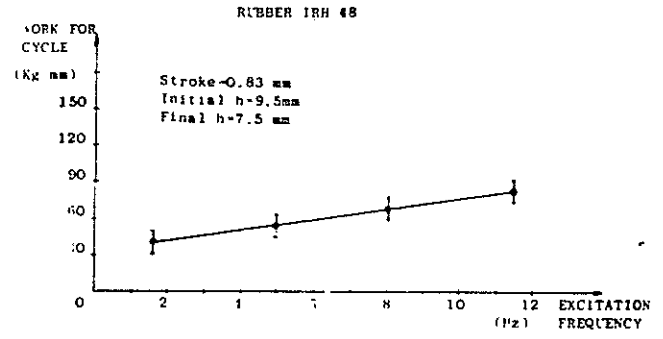
RUBBER IRH 48
WORK FOR CYCLE (Kg mm)
Stroke=0.83 mm
Initial h=9.5mm
Final h=7.5 mm
150
120
90
60
0
2
8
10
12
EXCITATION FREQUENCY (Hz)

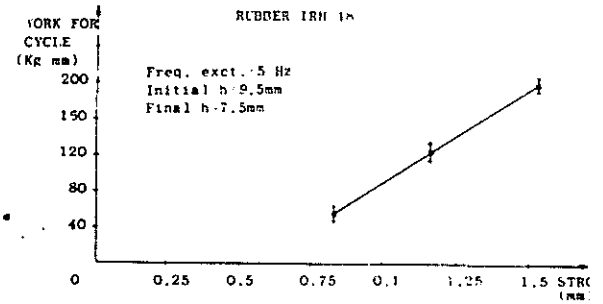
RUBBER IRH 18
WORK FOR CYCLE (Kg mm)
Freq. exct.=5 Hz
Initial h=9.5mm
Final h=7.5mm
200
150
120
80
40
0
0.25
0.5
0.75
1.25

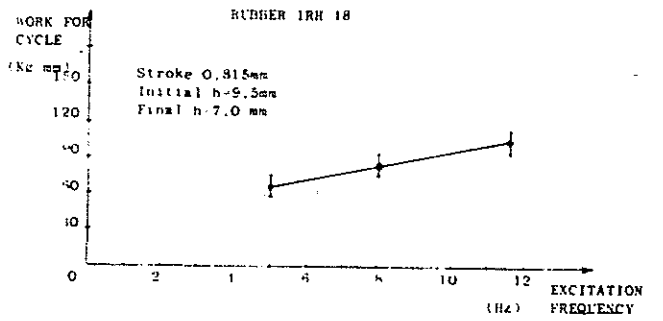
RUBBER IRH 18
WORK FOR CYCLE (Kg mm)
Stroke 0.815mm
Initial h=9.5mm
Final h=7.0 mm
120
0
2
10
12
EXCITATION FREQUENCY (Hz)

Fig. 20

Data listed refere to low frequency tests(up to 15Hz) this being the range where the phenomenon of mechanical instability appears and where also the elastomeric damper appears to be non linear.
Stable values are reached only when excitation frequency is above 20 ÷ 25 Hz.
Variations of K' and c/c_{cr} with frequency for different displacement amplitudes compression stresses and rubber hardness are shown in fig. (19).
The total error to be accounted for in these measurements is 4 ÷ 5% for K' and 8 ÷ 9% for c/c_{cr}.
Hysteresis cycles, corresponding to the work done at every cycle, for various amplitudes, frequencies and compression stresses are shown in fig. (18a-d).
The error here is about 4 ÷ 5%.
Fig. (19b) shows that, at constant frequency, dynamic stiffness increases as amplitude, hardness and compression decrease.
From the d f Fig. (19a) it is obviously not possible t te how damping ratio changes with the other parameters. These tests ought to be extended to other types of rubber. Considering the hysteresis cycles Fig. (18) and Fig. (20) it can be seen that for the rubber having an IRH of 48, an increase in compression of the material (each layer having been "squeezed" from a thickness of 9.5 mm. to 7.5 mm. and 9.5 mm. to 7 mm.) causes an increase of 45% in the work done per each cycle).
Damping ratio, though, remains the same.
On the other hand, work per cycle increases with frequency. Test results show also that, with a compressio of 2 mm for each layer (passing from 9.5 to 7.5 mm), work per cycle relative to the rubber with IRH = 55 is essentially the same as for the rubber with IRH = 48.
For a further compression of 0.5 mm (from 7.5 to 7.0) the work per cycle done by the 55 IRH rubber decreases. This is due to the fact that the layers of elastomeric material have been excessively compressed with regard to hardness.

CONCLUSIONS

The utility of using simultaneously the direct integration method, which permits the use of variable coefficients and the simulation of the dynamics of landing, and the method of Floquet has been demonstrated. The good results obtained in the simulation of hydraulic damper, the interesting behaviour of the elastomeric materials, the bad effects of play in mechanical coupling at the extremities of the damper, have lead us to think of a damper with a hydraulic piston, without calibrated valves but with an open orifice coupled to the struc e via elastomeric material. The characteristics elastomeric parts can be suitably modified for optimum cycle efficiency.

REFERENCES

1) Coleman, R.P., and Feingold, A.M. - THEORY OF SELF-EXCITED MECHANICAL OSCILLATIONS OF HELICOPTER ROTORS WITH HINGED BLADES - NACA TR1351, 1958.

2) Gabel, R. and Capurso, V. - EXACT MECHANICAL INSTABILITY BOUNDARIES AS DETERMINED FROM THE COLEMAN EQUATIONS - Journal of the American Helicopter Society, Vol.7, No.1, January 1962.

3) Hammond, C.E. - AN APPLICATION OF FLOQUET THEORY TO PREDICTION OF MECHANICAL INSTABILITY. - Journal of the American Helicopter Society, Vol.19, No.4, October 1974.

4) Potter, J.L. - IMPROVING RELIABILITY AND ELIMINATIN(NANCE WITH ELASTOMERIC DAMPERS - Journ: e American Helicopter Society, Vol.18, No.1, January 1973.

5) McGuire D.P. - THE APPLICATION OF ELASTOMERIC LEAD - LAG DAMPERS TO HELICOPTER ROTORS - Lord Library, 1975.

6) Barone - LA GOMMA ANTIVIBRANTE - S.A.G.A. publication - Milan, March 1970.

APPENDIX A

In general in the study of Ground Resonance the characteristics of the damper are considered to be linear even if these are non linear. For small oscillations of a helicopter the non-linear damper can be substituted by an equivalent linear one. In such a case the coefficients of stiffness and damping depend on the amplitude and frequency of the vibration. In particular, it is considered as an equivalent damper that, in one period, absorbs the same energy of a real damper at the same frequency and displacement amplitude of the piston rod. The force of reaction of the piston rod of an h au- lic damper can be expressed as:

$$F_R = \sigma \cdot V_{pist}^2 + P_o \qquad (7)$$

where

σ = Coefficient of hydraulic resistance

V_{pist} = Velocity of the piston (ωx_o)

Po = Coulombian force of friction

We can now write the equation for the motion of the piston as:

$$x = x_o \cdot \sin(\omega t)$$

then the energy absorbed per cycle by the real damper is,

$$L = 4 P_o x_o + \frac{8}{3} \sigma \omega^2 x_o^3 \qquad (8)$$

For a viscous damper eqn: (7) becomes:

$$F_R = C_{eq} \cdot V_{pist}$$

The energy absorbed by an equivalent viscous damper is:

$$L_1 = \pi C_{eq} \omega x_o^2$$

and equating this with equation (8) we get, Ceq, the equivalent viscous damping coefficient of the hydraulic damper:

$$C_{eq} = \frac{4}{\pi}\left(\frac{P_0}{\omega X_0} + \frac{2}{3}\sigma\omega X_0\right)$$

The behaviour of this coefficient for a certain value of σ and varying the maximum amplitude Xo is shown in fig.21.
We notice the independence of the minimum values of Ceq from the frequency.
There normally exists a limitation of the reaction forces using a system of **value** which impose that a required maximum value of the force of resistance cannot be exceeded; when $\sigma V_{pist}^2 + P_0$ exceeds the limiting value of the force, σ should vary as $1/V_{pist}^2$ so as to mai[illegible]e constancy of force F_R.
The effect o[illegible]nitation of the valves on the variation of Ceq as a function of the displacement of the piston rod is shown in figure 22. This behaviour is always with respect to a predetermined value of σ and the curves are drawn for different values of the frequency.
A variation of the orifice diameter brings in a variation of the coefficient (of proportionality) and this is obtained by the following considerations.
Let us express the reaction on the piston rod of the damper as

$$F = S.\Delta p = \sigma V_{pist}^2$$

where

S = Useful section of the Piston

Δp = Pressure loss across the orifice (difference of pressure between the two chambers of the damper)

V_{pist} = histantaneous velocity of the piston

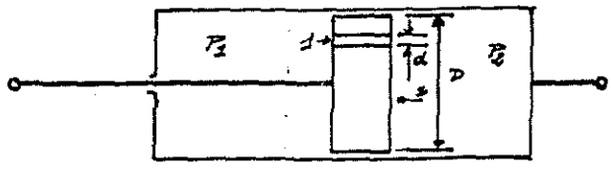

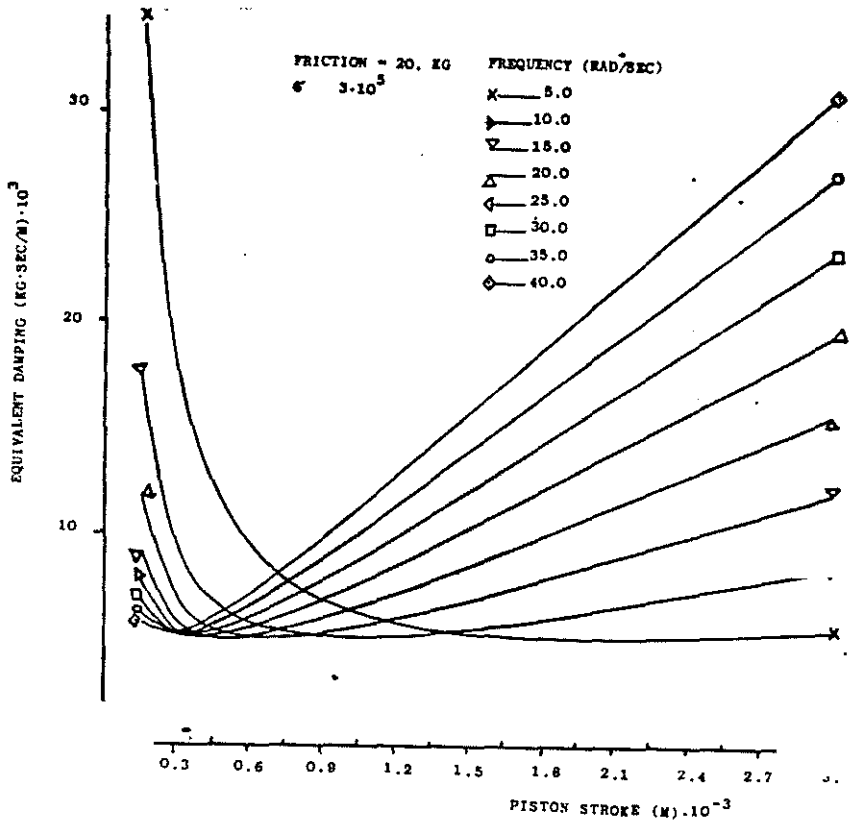
FRICTION = 20. KG
FREQUENCY (RAD/SEC)
5.0
10.0
15.0
20.0
25.0
30.0
35.0
40.0
EQUIVALENT DAMPING (KG·SEC/M)·10³
PISTON STROKE (M).10⁻³

Fig. 21

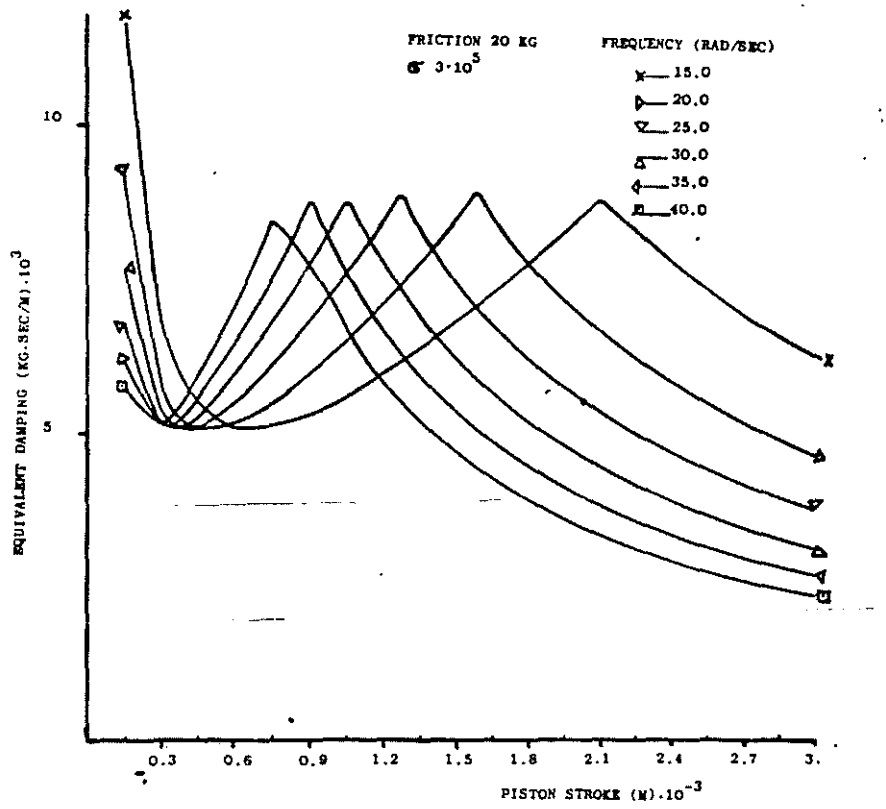
FRICTION 20 KG
FREQUENCY (RAD/SEC)
15.0
20.0
25.0
30.0
35.0
40.0
EQUIVALENT DAMPING (KG.SEC/M).10³
PISTON STROKE (M).10⁻³

Fig. 22

The flow across the orifice is:

$$q = C_{eff} \cdot s \cdot \sqrt{\frac{2\Delta p}{\rho}}$$

where

Ceff = Flow coefficient

s = Surface area of the orifice

Δp = Pressure loss

ρ = Density of fluid

Equating this flow with that resulting from the char in volume in Unit time by the motion of the piston we get,

$$\Delta p = \frac{V_{pist}^2 \cdot s^2 \cdot \rho}{2 \cdot C_{eff}^2 \cdot s^2}$$

Substituting Δp in equation (9) we have,

$$T = \frac{\varepsilon s^3 f}{\pi^2 C_{eff}^2 d^4}$$

The variation of the equivalent damping as a function of the displacement of the piston rod for fixed values of the force of friction, Piston rod stroke frequency; diameter of the orifice and T, for various values of the shear force is shown in figure 23.
The effect of variation of the diameter of the orifice, maintaining the shear force constant, on the coefficient of equivalent viscous damping is obtained by substituting the value of T which is related to the diameter in question as in equ: (9)

$$C_{eq} = \frac{1}{\pi}\left(\frac{P_0}{V_{pist}} + \frac{2}{3} V_{pist} \frac{\varepsilon s^3 f}{\pi \cdot C_{eff}^2 d^4}\right)$$

(it is assumed that Ceff is constant for small variations of diameter 'd') and which is shown in figures 24-25.

For $s = 0.003316\ m^2$

$\rho = 87.66\ Kg\ sec^2\ m^{-4}$

Ceff is 0.8.

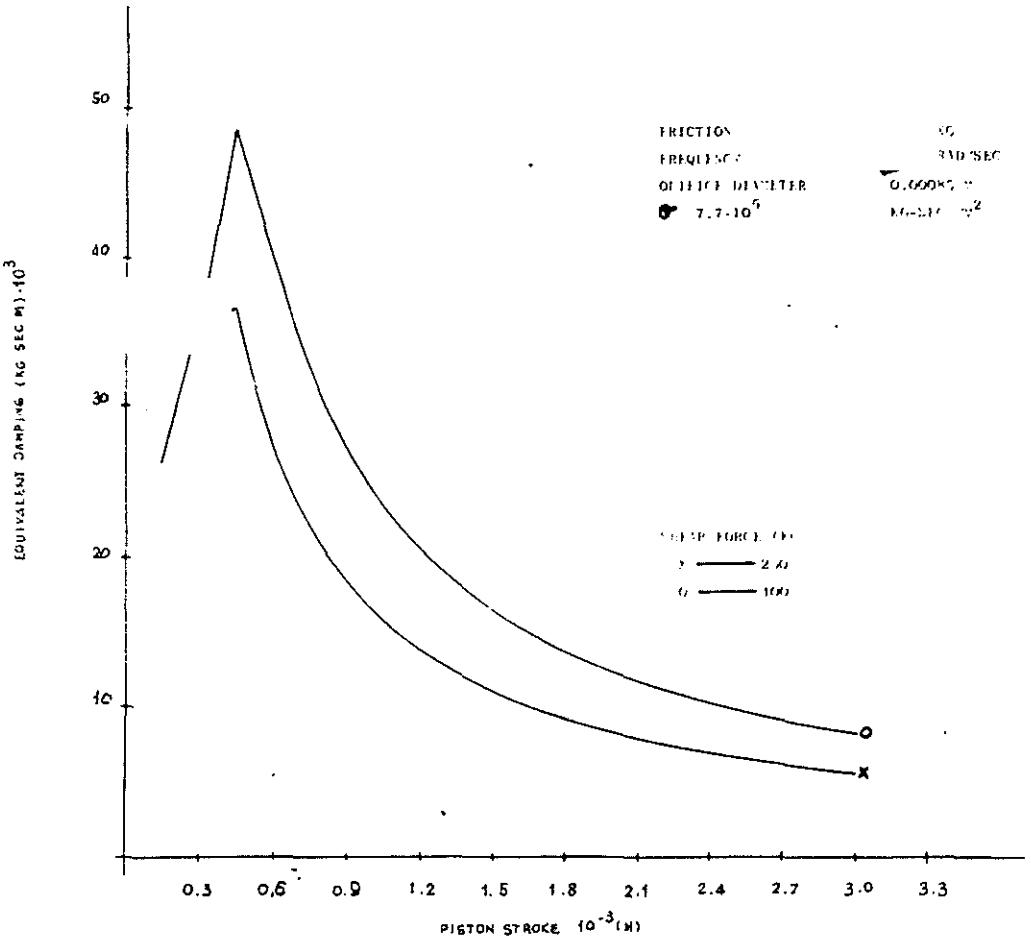
50
40
30
20
10
0.3
0,6
0.9
1.2
1.5
1.8
2.1
2.4
2.7
3.0
3.3
PISTON STROKE 10^{-3}(M)
EQUIVALENT DAMPING (KG SEC M)·10^{3}
FRICTION
$7.7 \cdot 10^{5}$

Fig.2

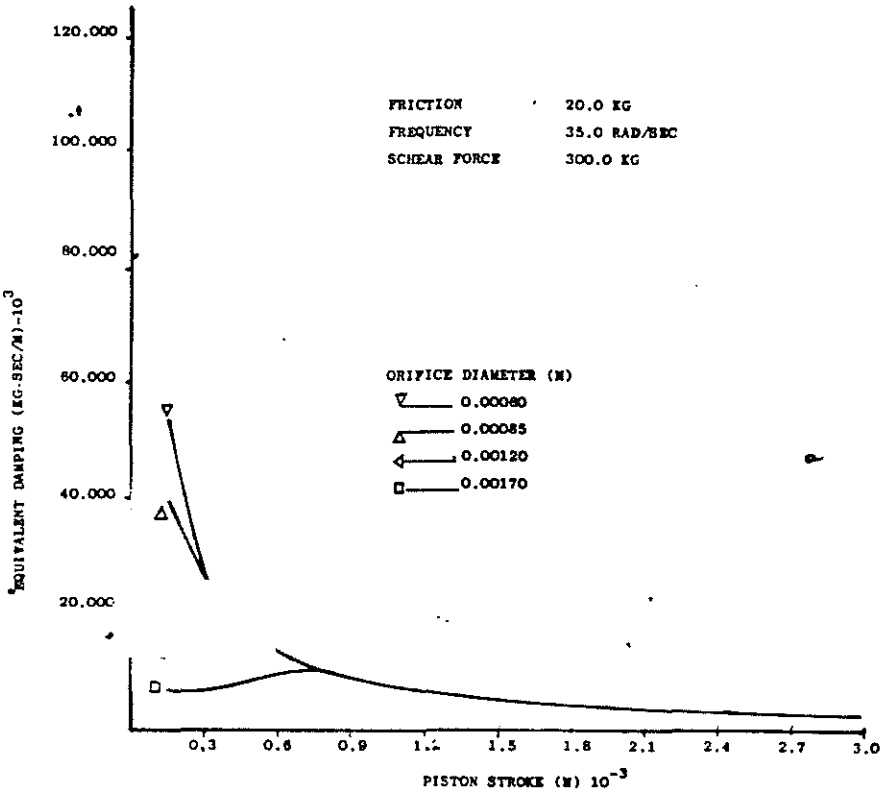
120.000
100.000
80.000
60.000
40.000
20.000
EQUIVALENT DAMPING (KG-SEC/M)-10^{3}
FRICTION 20.0 KG
FREQUENCY 35.0 RAD/SEC
SHEAR FORCE 300.0 KG
ORIFICE DIAMETER (M)
0.00080
0.00085
0.00120
0.00170
0.3 0.6 0.9 1.2 1.5 1.8 2.1 2.4 2.7 3.0
PISTON STROKE (M) 10^{-3}

Fig.24

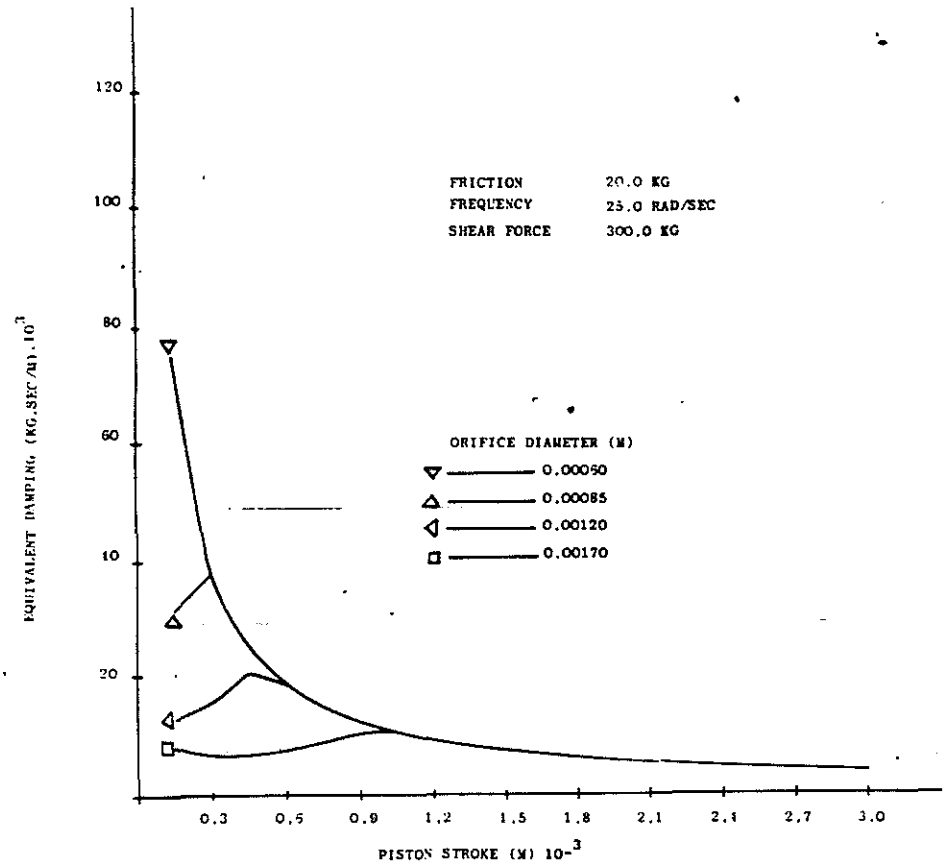
120
100
80
60
10
20
FRICTION 20.0 KG
FREQUENCY 25.0 RAD/SEC
SHEAR FORCE 300.0 KG
ORIFICE DIAMETER (M)
0.00050
0.00085
0.00120
0.00170
0.3 0.6 0.9 1.2 1.5 1.8 2.1 2.4 2.7 3.0
PISTON STROKE (M) 10^{-3}

Fig.25

In particular, one can notice the effect of frequency by a comparison of the 2 figures.
The same behaviour can be shown in a common diagram if we consider the velocity of the piston as independent variable instead of the displacement (see figur: 26.

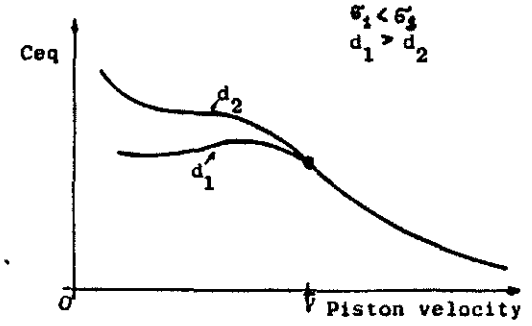

Fig.26

It is observed that, for $V_{pist} < \overline{V}$ an increase in the diameter of the orifice reduces Ceq.
For $V_{pist} > \overline{V}$ there is no variation of Ceq.
Also, it is noted that, as the diameter of the orifice increases the value of $\overline{V}$ increases after which we have no variation of Ceq (as function of V pist).
Figure 27 shows how the increase in the diameter of the orifice modifies the Force-V_{pist} diagram

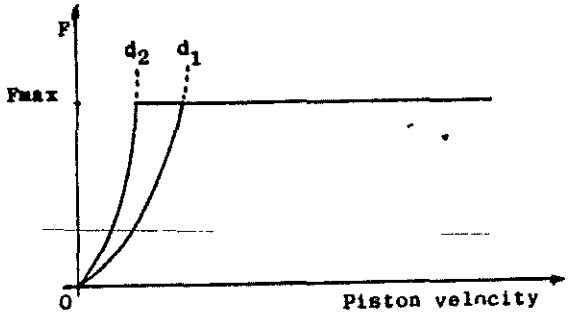

(Figure 27)

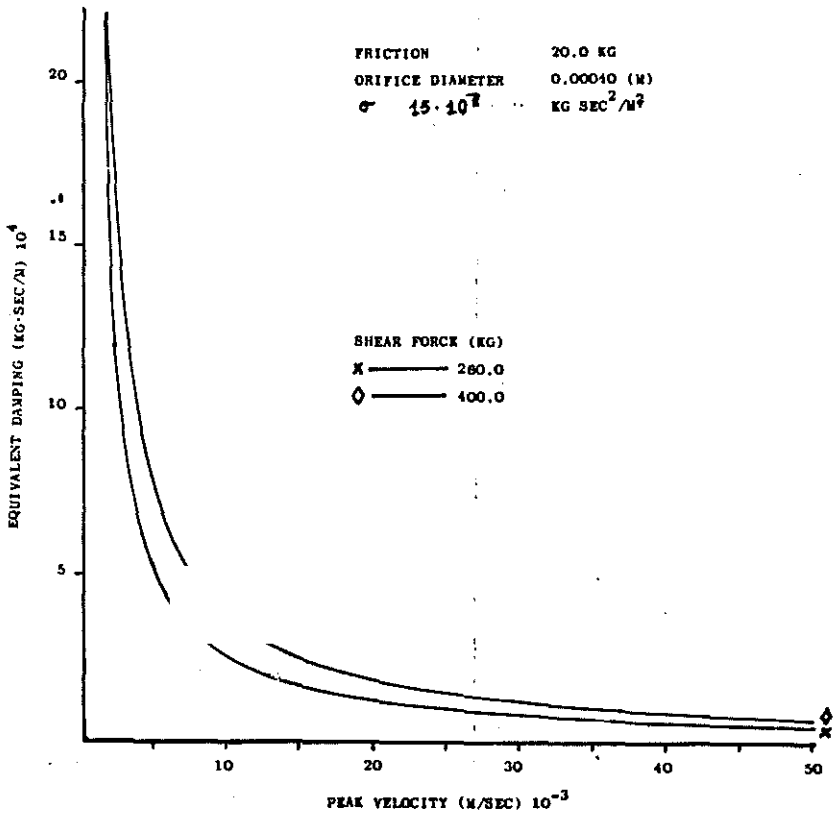
FRICTION 20.0 KG
ORIFICE DIAMETER 0.00040 (M)
σ 15·10⁷ KG SEC²/M²
SHEAR FORCE (KG)
X 280.0
◊ 400.0
EQUIVALENT DAMPING (KG·SEC/M) 10⁴
PEAK VELOCITY (M/SEC) 10⁻³

Fig. 28

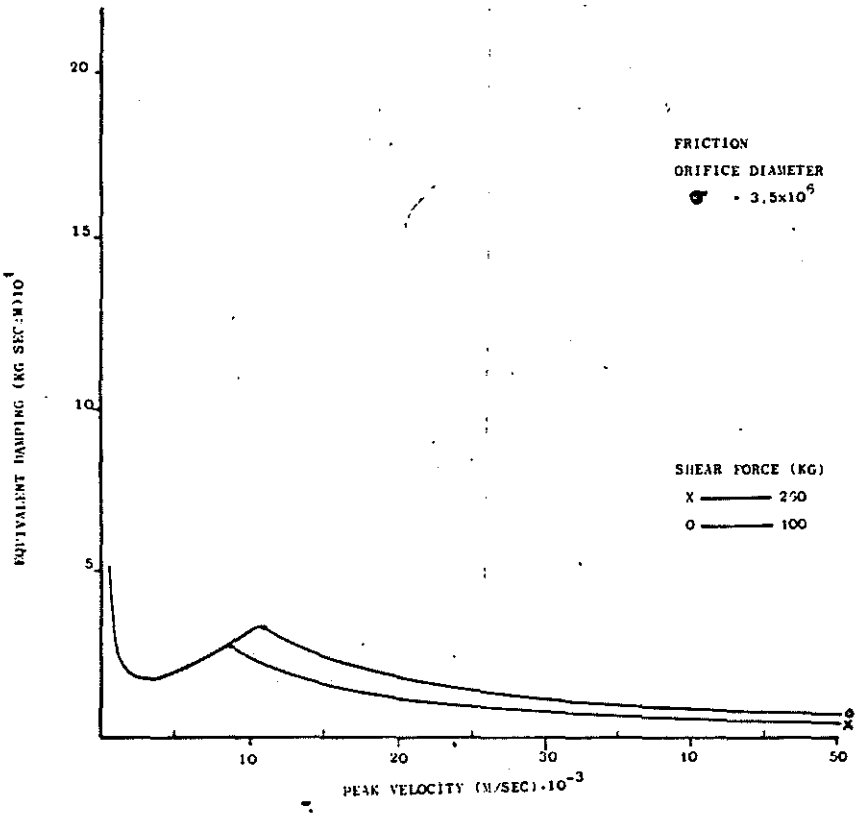
FRICTION 20.0 KG
ORIFICE DIAMETER 0.00101 M
σ 3.5x10⁶ KG SEC²/M²
SHEAR FORCE (KG)
X 280
O 100
EQUIVALENT DAMPING (KG SEC/M)10⁴
PEAK VELOCITY (M/SEC)·10⁻³

Fig. 29

The effect on the Ceq due to an increase in the Shear force at constant orifice diameter is illustrated in figures 28 and 29.
Results of numerous experiments conducted have confirmed this fact.
The conclusion that one can draw as regards the behaviour of Ceq, as a function of the velocity V_{pist} of the piston rod of the damper are:

1) The variation of Ceq as a function of the physical and geometrical parameters for a damper like the one we have considered, confirms the interest for the use of the methods of investigation which take note of the non-linearit
2) At very low velocity the effect of frictio_ _ fundamental.
3) The middle part of the curve is characterized by the orifice diameter; the maximum peak is a ɔn of the shear force.
4) T_ _ _ _ part tapers off, is not depende on the geometry of the orifice but only on the value of the shear force.